UNIVERSITAT POLITÈCNICA DE CATALUNYA
BARCELONATECH
Escola Tècnica Superior d'Enginyeria
de Telecomunicació de Barcelona

telecos
BCN

Quantum Simulation

Bachelor's Degree Thesis
Submitted to the Faculty at the
Escola Tècnica Superior
d'Enginyeria de Telecomunicació de Barcelona
of the Universitat Politècnica de Catalunya
by

Albert López Escudero

In partial fulfillment
of the requirements for the
Degree in Electronics Engineering

Advisor: Vincenzo de Maio & Ivona Bandric
Reviewer: Javier Rodrigez Fonollosa

Barcelona, January 2025

ETSETB – Degree in Electronics Engineering

Resum

Cada exemplar del Treball de Fi de Grau (TFG) ha de contenir un Resum, que és un breu extracte del TFG. En termes d'estil, el Resum hauria de ser una versió reduïda del projecte: una introducció concisa, un compendi dels resultats i les principals conclusions o arguments presentats en el projecte. El Resum no ha de superar les 150 paraules i cal que estigui traduït al català, castellà i anglès.

Resumen

Cada ejemplar del Trabajo de Fin de Grado (TFG) debe incluir un Resumenque es un breve extracto del TFG. En cuanto al estilo, el Resumen debería ser una versión reducida del proyecto: una introducción breve, un resumen de los resultados principales y las conclusiones o argumentos principales presentados en el proyecto. El Resumen no debe exceder las 150 palabras y debe estar traducido al catalán, castellano e inglés.

Summary

Each copy of the Bachelor's Thesis (TFG) must include a Summary, which is a concise abstract of the TFG. In terms of style, the Summary should be a condensed version of the project: a brief introduction, a summary of the main results, and the conclusions or key arguments presented in the project. The Summary should not exceed 150 words and must be translated to catalan, spanish and english.

A Dedication page may be included in your thesis just before the Acknowledgments page, but it is not a requirement.

Acknowledgements

It is appropriate, but not mandatory, to declare the extent to which assistance has been given by members of the staff, fellow students, technicians or others in the collection of materials and data, the design and construction of apparatus, the performance of experiments, the analysis of data, and the preparation of the thesis (including editorial help). In addition, it is appropriate to recognize the supervision and advice given by your advisor.

Revision history and approval record

Revision	Date	Author(s)	Description
1.0	dd/mm/yyyy	AME	Document creation
1.1	dd/mm/yyyy	AME, JPV	Error correction
2.0	dd/mm/yyyy	AME, MLO	Revised after review
4.0	dd/mm/yyyy	AME	Final version

DOCUMENT DISTRIBUTION LIST

Role	Surname(s) and Name
[Student]	
[Project Supervisor 1]	
[Project Supervisor 2 (if applicable)]	

Written by:		**Reviewed and approved by:**	
Date	dd/mm/yyyy	Date	dd/mm/yyyy
Name	Xxxxxxx Yyyyyyy	Name	Xxxxxxx Yyyyyyy
Position	Project Author	Position	Project Supervisor

Contents

List of Figures

List of Tables

Abbreviations

Adagrad Adaptive Gradient Algorithm

Adam Adaptive Moment Estimation

ADAPT-VQE Adaptive Variational Quantum Eigensolver

AQS Analog Quantum Simulation

CCSD Coupled Cluster with Singles and Doubles

CPU Central Processing Unit

DQS Digital Quantum Simulation

ETSETB Escola Tècnica Superior d'Enginyeria de Telecomunicació de Barcelona

EU European Union

FCI Full Configuration Interaction

GD Gradient Descent

GEF Grau en Enginyeria Física

GPU Graphics Processing Unit

GREELEC Grau en Enginyeria Electrònica de Telecomunicació

HF Hartree-Fock

MPS Matrix Product States

NISQ Noisy Intermediate-Scale Quantum

NMomentum Nesterov Momentum

PEPS Projected Entangled Pair States

QNG Quantum Natural Gradient

RMSProp Root Mean Square Propagation

UCCSD Unitary Coupled Cluster with Singles and Doubles

VQE Variational Quantum Eigensolver

CHAPTER 1

Introduction

In recent years, we have witnessed a technological revolution. Devices have evolved at an extraordinary pace, reaching a level of sophistication that has brought computing to a point where improving the hardware of traditional devices presents significant challenges.

This improvement has been achieved, in part, through the reduction in the size of transistors, a principle described by Dennard Scaling in 1974. This principle indicates that by reducing the size of transistors, both their performance and efficiency are improved. Additionally, an important empirical observation is Moore's Law, which states that the number of transistors in a microprocessor doubles every two years.

These two phenomena have led to exponential growth in processing capacity.Nevertheless,physical and technological limitations have halted the ability to further reduce the size of transistors. For this reason, research into alternatives to classical computing has become one of the main objectives for many companies today.

It has been observed that quantum computing is particularly effective in certain fields, one of which is quantum simulation. In this project, we will use quantum computing to simulate molecular systems, focusing on achieving efficient and precise quantum simulations. To this end, advanced methodologies have been implemented to improve efficiency and resource utilization on a classical computer, and the Variational Quantum Eigensolver (VQE) algorithm has been employed, which will be explained in greater detail later.

1.1 Work goals

The main objective of our project has been to develop a method to parallelize evaluations of quantum molecular dynamics simulations. To this end, the following objectives have been declared:

- Optimize the quantum simulation framework to minimize computational overhead while maintaining accuracy in modeling molecular systems.

- Integrate an adaptive quantum ansatz capable of dynamically selecting and integrating operators with the highest impact on performance, ensuring rapid convergence and reduced computational cost.
- Integrate advanced hybrid optimization cycles that streamline both electronic state and nuclear geometry refinements, with an emphasis on computational speed and scalability.
- Design a high-performance, modular architecture tailored for extensibility, facilitating the efficient inclusion of ansatz designs, optimization strategies and different types of molecules.

1.2 Requirements and specifications

To achieve these objectives, the following requirements and specifications have been established:

- **Dynamic Quantum Circuit Construction**: Integrate an adaptive quantum circuit mechanism that employs energy gradient calculations to iteratively select and include the most impactful operators, reducing the complexity of the quantum circuits without compromising accuracy.
- **Advanced Hybrid Optimization**: Develop a unified optimization cycle combining variational parameter updates and nuclear geometry refinements, supported by precise gradient-based techniques. Ensure the use of optimizers for rapid convergence and enhanced stability.
- **Scalable System Representation**: Implement a modular system construction process that accommodates different molecular geometries and basis sets with efficient computation of molecular properties.
- **Efficient Gradient Computation**: Optimize gradient calculations for both quantum and nuclear coordinates using automatic differentiation, enabling simultaneous updates and faster convergence.
- **Performance Monitoring and Visualization**: Develop tools for tracking energy convergence, execution time, and molecular geometry evolution. Include detailed visualizations (e.g., energy evolution plots, 3D geometries) to ensure transparency and allow performance analysis.
- **Extensibility and Modularity**: Ensure a modular project structure that facilitates the inclusion of new ansatz types, optimizers, and molecular systems with minimal adjustments. Employ a structured directory for clear separation of functionality and scalability.
- **Parallel Execution Capability**: Leverage multiprocessing capabilities to evaluate multiple optimizers and configurations in parallel, enabling comprehensive performance analysis across various configurations.

1.3 Methods and procedures

To achieve the objectives of this project, we carried out a series of implementations to achieve the previously mentioned objectives. As an initial phase, the existing frameworks currently on the market were compared to begin the development of our project. Next, a first, basic version was developed to simulate a single molecule with a single configuration.

In the first version of the project, a single quantum simulation was developed with the aim of verifying that the framework worked correctly and allowed us to use it for our project. Once this was verified, the next step was to begin developing the modular structure of the project, which would facilitate the integration of new components into our project. This modular structure would allow us to compare the different components of our quantum molecular dynamics simulator.

Subsequently, a series of techniques were implemented, integrating quantum classical algorithms, to find the lowest energy values in our simulations. Additionally, the integration of the modular structure facilitated the implementation of configurations for our simulations, allowing us to make different configurations and thus find these minimum values more efficiently.

By modularizing the project, it became possible to parallelize different simulation configurations, as by modifying the variable values, we could simulate different molecules and internal configurations of the optimizer.

Finally, tools were implemented to visualize the results and store them automatically and easily. These results are especially important as they allow us to analyze the obtained data in greater depth, enabling us to draw more precise conclusions.

1.4 Work plan

During the development of the project, the initial plan was largely followed. However, several complications arose that extended some deadlines, requiring adjustments to the overall timeline to achieve the established objectives.

The main setback was related to the integration of the JAX interface. From the outset, we were confident that using JAX would significantly improve the performance of the simulations. However, upon completing the initial integration, we were surprised to find that the performance not only failed to improve but actually worsened. This unexpected result led us to conduct more checks than initially planned, aiming to verify the accuracy of the results and identify the root cause of this behavior.

This situation caused delays in the second phase of the project, which, in turn, required a reduction in the time allocated to the third phase to meet the deadlines. Despite this, we decided not to compromise on the quality of the project. As a result, the overall development time had to be extended, increasing the daily hours dedicated to the project. This additional effort ensured that the initial objectives were achieved without compromising

the proposed quality standards.

GANTT DIAGRAM

QUANTUM SIMULATIONS		UNIVERSITY	TU WIEN
ALBERT López Escudero		DATE	04/10/24

WP	TITLE OF THE WORK	START DATE	DELIVERY DATE	DURATION
1	**Initial Phase**			
1.1	T1	01/10/24	20/10/24	19
1.2	T2	07/10/24	27/10/24	20
1.3	T3	20/10/24	25/10/24	5
2	**Second Phase**			
2.1	T4	25/10/24	07/11/24	12
2.2	T5	08/11/24	25/11/24	17
2.3	T6	08/11/24	30/11/24	22
2.4	T7	25/11/24	30/11/24	5
3	**Final Phase**			
3.1	T8	01/12/24	20/12/24	19
3.2	T9	15/12/24	31/12/24	16
3.3	T10	01/01/25	15/1/25	14
3.5	T11	01/01/25	15/1/25	14
3.4	T12	01/01/25	19/1/25	18
Meetings				

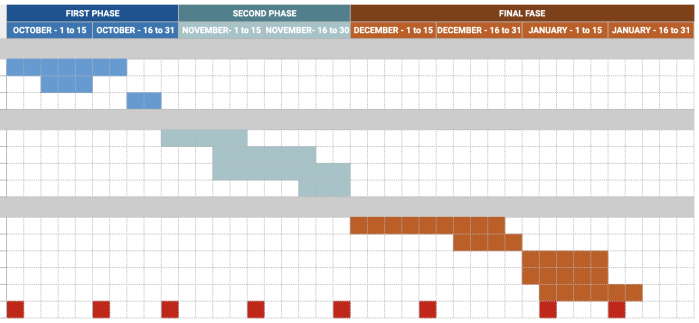

Figure 1.1: *Gantt diagram showing the project timeline and the distribution of tasks over the development period.*

CHAPTER 2

State of the Art

In this project, we focus on the operation of quantum simulators applied to molecular simulation, an area where quantum computing offers significant advantages. The main objective is to develop a program capable of simulating different molecules in a simple and efficient manner.

To this end, we will review the basic concepts of quantum mechanics that are essential to understand the fundamentals and potential of quantum computing, and explore the techniques of quantum simulation that allow us to harness quantum computing capabilities even with current technological limitations.

2.1 Quantum Computing

It is essential to understand the difference between bits in classical computing and qubits in quantum computing to delve into this new technological paradigm.

In classical computing, the basic unit of information is the **bit**, which can take the value of 0 or 1. These bits are the foundation upon which conventional computers operate, processing information through combinations of these binary states.

In contrast, quantum computing uses the **qubit** or quantum bit as its basic unit. Unlike the classical bit, a qubit can exist in a superposition of states, meaning it can simultaneously represent the values 0 and 1 thanks to the principle of superposition in quantum mechanics. This property, along with phenomena such as quantum entanglement and interference, allows quantum computers to process information exponentially more efficiently for certain problems.

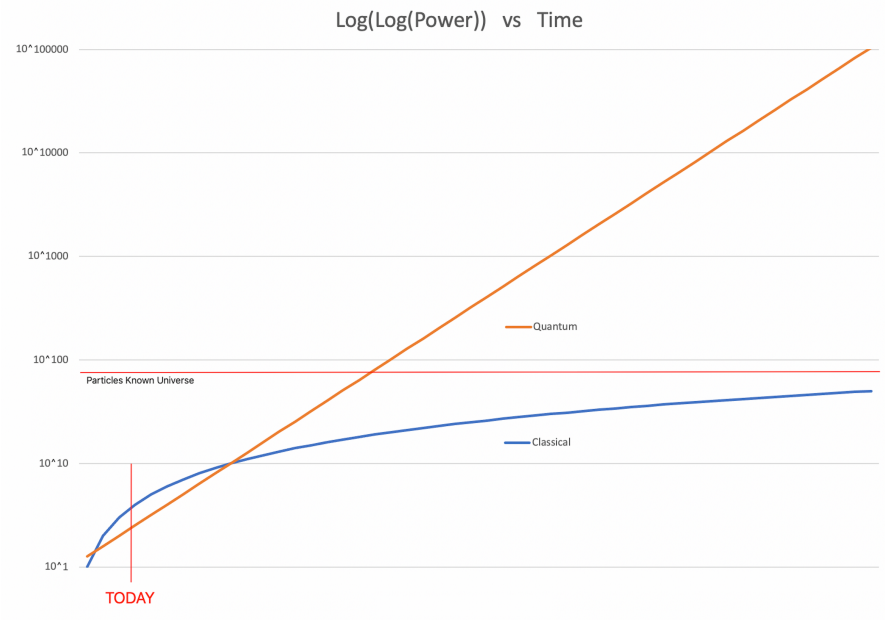

Figure 2.1: *Comparison between the growth of classical and quantum computational capacity.[24]*

This graph shows us the boundaries that quantum computing allows us to reach compared to classical computing. It could achieve and dramatically surpass computational power.

Understanding how qubits operate and their differences from classical bits is essential to understand the potential of quantum computing. For this reason, the fundamental concepts of quantum computing are presented below.

2.1.1 Qubit

The **qubit** is the basic unit of information in quantum computing. While the classical bit can only be in one of two states (0 or 1), a qubit can be in a superposition of both states simultaneously. This is due to the principle of quantum superposition, one of the fundamental characteristics of quantum mechanics. It is worth noting that the states of a system are usually described by vectors, which reside in a Hilbert space.

For qubits, the Hilbert space is 2-dimensional, and the following values can be taken:

- $|0\rangle$: Represents the basis state 0.

$$|0\rangle = \begin{pmatrix} 1 \\ 0 \end{pmatrix}$$

- $|1\rangle$: Represents the basis state 1.

$$|1\rangle = \begin{pmatrix} 0 \\ 1 \end{pmatrix}$$

Mathematically, a qubit is represented as a linear combination of the basis states $|0\rangle$ and $|1\rangle$:

$$|\psi\rangle = \alpha\,|0\rangle + \beta\,|1\rangle$$

where α and β are complex numbers that satisfy the normalization condition $|\alpha|^2+|\beta|^2 = 1$. These coefficients indicate the probability amplitudes of finding the qubit in the states $|0\rangle$ or $|1\rangle$ upon measurement.[22]

2.1.2 Quantum Entanglement

An important distinguishing feature between qubits and classical bits is that multiple qubits can exhibit **quantum entanglement**; the qubit itself is an exhibition of quantum entanglement. In this case, quantum entanglement is a local or nonlocal property of two or more qubits that allows a set of qubits to express higher correlation than is possible in classical systems.

The simplest system to display quantum entanglement is the system of two qubits. Consider, for example, two entangled qubits in the $|\Phi^+\rangle$ Bell state:

$$|\Phi^+\rangle = \frac{1}{\sqrt{2}}\big(\,|00\rangle + |11\rangle\,\big).$$

There are equal probabilities of measuring either product state $|00\rangle$ or $|11\rangle$, this is called **equal superposition**:

$$\left|\frac{1}{\sqrt{2}}\right|^2 = \frac{1}{2}.$$

In other words, there is no way to tell if the first and the second qubit has value 0 or 1.

To better understand quantum entanglement, let's explain an example. Imagine these qubits are separated, with one qubit given to Alice and the other to Bob. Alice performs a measurement, and the result she obtains has equal probabilities for both $|0\rangle$ and $|1\rangle$. If Bob measures the value of his qubit at the same time, the result must be exactly the same due to quantum entanglement.

If Alice's measurement had been $|0\rangle$, then Bob's result would also have been $|0\rangle$, because $|00\rangle$ is the only state where Alice's qubit is $|0\rangle$. In short, for these two entangled qubits, whatever Alice measures, so does Bob, demonstrating perfect correlation in any basis, regardless of the distance between them. This is a surprising phenomenon that cannot be explained by classical physics.[14]

2.1.3 Quantum Superposition

Quantum superposition allows a quantum system to exist in multiple states simultaneously until a measurement is performed. This characteristic is key to the functioning of quantum computers, as it enables processing a large amount of inputs simultaneously.

A qubit, by itself, is not much more powerful than a conventional bit. What makes it truly powerful is that it can place the quantum information it holds into a state of superposition, which represents a combination of all possible configurations of the qubit. Groups of qubits in superposition can create complex, multidimensional computational spaces, allowing complex problems to be represented in new ways within these spaces.[10]

Superposition is especially useful in simulating complex molecular systems. Quantum computers can naturally model the superpositions of electronic states in molecules, which is crucial for studying chemical reactions and molecular properties that are difficult to address with classical methods due to the exponential growth of computational resources required.

2.1.4 Quantum Decoherence

Quantum decoherence is one of the main challenges in quantum computing. Such machines are expected to rely heavily on the undisturbed evolution of quantum coherence. Decoherence causes the system to lose its quantumness, which invalidates the superposition principle and turns quantum to classical behavior. They must handle the decoherence in order to maintain quantum computation performance.[26]

Qubits are extremely sensitive to external disturbances, such as electromagnetic fluctuations, vibrations, and temperature changes. These interactions can cause quantum states to mix with those of the environment, leading to a loss of coherence that is irreversible and degrades the stored quantum information.[27]

To mitigate the effects of decoherence, various strategies are implemented:

- **System Isolation**: Designing physical systems that minimize unwanted interactions with the environment, using materials and techniques that protect qubits from external disturbances.
- **Quantum Error Correction**: Implementing error correction codes that allow detecting and correcting errors without directly measuring the qubit's state, thereby preserving quantum information.
- **Dynamic Control**: Applying techniques such as pulse refocusing and dynamic pulse sequences that actively compensate for disturbances and extend the coherence time of qubits.

Controlling and mitigating decoherence are essential for the advancement of quantum computing and its application in areas like molecular simulation, where the precision of calculations is fundamental.

2.2 Quantum Simulation

Quantum simulation has become a vital tool for investigating intricate quantum systems that are beyond the reach of classical computational methods. Building on Richard

Feynman's idea that a computer operating on quantum principles could exceed the capabilities of classical machines for modeling quantum behavior, the field has seen rapid advancements. Today, it spans both digital and analog approaches and finds applications in numerous scientific domains.

There are mainly two approaches in quantum simulation: **Digital Quantum Simulation (DQS)** and **Analog Quantum Simulation (AQS)**. DQS employs quantum circuit models to study the dynamics of the system, thus emulating, with the help of qubits, the behavior of the system. This approach is universal, as it can, in principle, simulate any quantum system, although not always efficiently. On the other hand, AQS uses an accessible quantum system to emulate the Hamiltonian of the system, thereby allowing us to learn about the properties of the system we want to study. This method is particularly useful when a qualitative representation is required rather than high precision.[8]

In addition to these approaches, there are algorithms inspired by quantum information theory that facilitate the classical simulation of quantum systems using the internal symmetries of particles. Techniques such as **Matrix Product States (MPS)** and **Projected Entangled Pair States (PEPS)** allow representing particle systems on classical computers more efficiently than standard classical methods, optimizing the calculation of properties of complex quantum systems. [2]

The applications of the quantum simulation systems are an exciting area of scientific practice. In condensed matter physics, it allows the study of models such as the Hubbard model and quantum phase transitions, fundamental for understanding phenomena like superconductivity, it facilitates the calculation of molecular energies and complex chemical reactions, it emulates particles in high-energy fields and cosmological phenomena. Furthermore, quantum simulation promises to have applications in the study of many problems; high-energy physics, atomic physics, quantum chemistry, condensed-matter physics and cosmology. This could be implemented using quantum computers, but also with simpler, analog devices that require less control and are, therefore, easier to construct.[4]

But there are still challenges to deal with. It's tough to control quantum simulator systems properly. Plus, errors and decoherence can degrade or adversely affect the results. The number of qubits and quantum gates we need depends on how big and complex the system is. We think you need around 40 to 100 qubits to beat classical computers on some problems. Despite these hurdles, tech is advancing, and we're getting better at quantum simulation. This could really change how we do research in science and help us learn more about the quantum world.

2.3 Hamiltonian

The Hamiltonian is a fundamental concept originating from classical mechanics, who developed a reformulation of Newtonian mechanics. Hamiltonian mechanics is a reformulation of classical mechanics that provides powerful tools for studying the dynamics of systems.

The Hamiltonian of a system represents the total energy of the system, expressed in terms of generalized coordinates and momenta, and is given by the sum of the kinetic and potential energies. The **Hamiltonian operator** plays a central role in describing the energy and time evolution of quantum systems, takes different forms and can be simplified, in some cases. It represents the total energy of the system, including kinetic and potential energies, being essential for formulating the Schrödinger equation.[7]

2.3.1 Mathematical Definition

The Hamiltonian operator, typically denoted as $\hat{H}$, is a self-adjoint operator acting on the Hilbert space associated with the quantum system. For a single particle in one dimension, the Hamiltonian is expressed as:

$$\hat{H} = \hat{T} + \hat{V}$$

where:

- $\hat{T}$ is the kinetic energy operator.
- $\hat{V}$ is the potential energy operator.

In terms of the position $\hat{x}$ and momentum $\hat{p}$ operators, these are defined as:

$$\hat{T} = \frac{\hat{p}^2}{2m} = -\frac{\hbar^2}{2m}\frac{d^2}{dx^2}$$

$$\hat{V} = V(\hat{x})$$

Here, m is the mass of the particle, $\hbar$ is the reduced Planck constant, and $V(\hat{x})$ is the potential energy function depending on position.

Finally, it can be shown that the expectation value of the Hamiltonian, which represents the energy expectation value, is always greater than or equal to the system's minimum potential:[7]

Computing the expectation value of the kinetic energy, we have:

$$\begin{aligned} T &= -\frac{\hbar^2}{2m}\int_{-\infty}^{+\infty} \psi^* \left(\frac{d^2\psi}{dx^2}\right) dx \\ &= -\frac{\hbar^2}{2m}\left(\left[\psi'(x)\psi^*(x)\right]_{-\infty}^{+\infty} - \int_{-\infty}^{+\infty} \left(\frac{d\psi}{dx}\right)\left(\frac{d\psi}{dx}\right)^* dx\right) \\ &= \frac{\hbar^2}{2m}\int_{-\infty}^{+\infty} \left|\frac{d\psi}{dx}\right|^2 dx \geq 0. \end{aligned}$$

Hence the expectation value of the kinetic energy is always nonnegative. We can calculate the expectation value of the total enegy for normalized wavefunction:

$$E = T + \langle V(x) \rangle = T + \int_{-\infty}^{+\infty} V(x)|\psi(x)|^2 \, dx \geq V_{\min}(x) \int_{-\infty}^{+\infty} |\psi(x)|^2 \, dx \geq V_{\min}(x).$$

2.3.2 Role in the Schrödinger Equation

The Hamiltonian is central to the Schrödinger equation, which describes how the quantum state of a system evolves over time. The time-dependent Schrödinger equation is expressed as:

$$i\hbar \frac{\partial}{\partial t} |\psi(t)\rangle = \hat{H}|\psi(t)\rangle$$

where $|\psi(t)\rangle$ is the state vector of the system at time t. For time-independent systems, the Schrödinger equation reduces to the eigenvalue equation:

$$\hat{H}|\psi\rangle = E|\psi\rangle$$

Here, E represents the energy level or eigenvalues of the state ψ , this equation is known as the *time-intependent Schrödinger equation.*[20]

2.3.3 Hamiltonian in Multi-Particle Systems

We can extend the concept of the Hamiltonian to systems with N particles.[7] The Hamiltonian is expressed as:

$$\hat{H} = \sum_{n=1}^{N} \hat{T}_n + \hat{V}$$

where:

- $\hat{V}$: is the potential energy function, which depends on the spatial configuration of the system and time. A particular set of spatial positions at a given instant defines a configuration.
- $\hat{T}_n$: is the kinetic energy operator for particle n, given by:

$$\hat{T}_n = \frac{\hat{\mathbf{p}}_n \cdot \hat{\mathbf{p}}_n}{2m_n} = -\frac{\hbar^2}{2m_n} \nabla_n^2$$

Combining these yields, the Schrödinger Hamiltonian for an N number of particles

system:

$$\begin{aligned}\hat{H} &= \sum_{n=1}^{N} \hat{T}_n + \hat{V} \\ &= \sum_{n=1}^{N} \frac{\hat{\mathbf{p}}_n \cdot \hat{\mathbf{p}}_n}{2m_n} + V(\mathbf{r}_1, \mathbf{r}_2, \ldots, \mathbf{r}_N, t) \\ &= -\frac{\hbar^2}{2} \sum_{n=1}^{N} \frac{1}{m_n} \nabla_n^2 + V(\mathbf{r}_1, \mathbf{r}_2, \ldots, \mathbf{r}_N, t)\end{aligned}$$

2.3.4 The second quantization

Finding an exact solution of the Schrödinger equation is equivalent to solving the Full Configuration Interaction (FCI) functions, where the wave function of a molecule is represented as a sum of all possible Slater determinants that can be formed using a specific set of molecular orbitals. As the number of electrons and orbitals increases, the number of Slater determinants grows exponentially, making the FCI method computationally infeasible for large systems. Therefore, it is recommended to use a quantum computer to solve this problem. For this reason, we need to transform the Hamiltonian to the second quantized operators' form.

For more than one particle, the secondquantized Hamiltonian can be written under the form:

$$H = \sum_{p,q} h_{pq} a_p^\dagger a_q + \sum_{p,q,r,s} h_{pqrs} a_p^\dagger a_q^\dagger a_r a_s,$$

with $a^\dagger$ and a being the electron creation and annihilation operators. The first term thus represents the transitions of single electrons between orbitals, while the second term corresponds to the interactions between pairs of electrons[1].

2.3.5 Importance in Quantum Simulations

In quantum simulations, especially in algorithms like the Variational Quantum Eigensolver (VQE), the Hamiltonian is decomposed into a sum of simpler terms, often expressed in terms of Pauli operators. This decomposition facilitates implementation on quantum circuits and allows estimating the system's energy through measurements on qubits.

Understanding the structure and properties of the Hamiltonian is essential for modeling and simulating quantum systems, as it determines the possible energies and dynamics of the system under study.

2.4 VQE: Variational Quantum Eigensolver

Variational quantum eigensolvers (VQEs) are among the most promising candidates for achieving useful computations in chemistry on near-term quantum computers. They

operate by varying parameters and optimizing them to achieve the lowest energy, this can be achived by using variational principle from quantum mechanics.

At their core, they prepare a quantum state, determined by a set of classical parameters that are specified by an *ansatz*, measuring its energy on the quantum computer. Then, a new quantum state is prepared with a new set of parameters, selected by any classical optimization algorithm, and the process is repeated until the energy is minimized. If the energy is carried out perfectly, we approximate this value to the ground-state energy. [18]

Among the hybrid quantum-classical algorithms developed to address quantum simulation challenges, the *Variational Quantum Eigensolver (VQE)* has gained particular relevance. That aims to solve for the ground state of a given Hamiltonian represented as a linear combination of Pauli terms, with an ansatz circuit where the number of parameters to optimize over is polynomial in the number of qubits. [16]

2.4.1 Fundamental Principles and Stages of the Algorithm

VQE is founded on the **variational principle** of quantum mechanics, which states that the expectation value of the energy $E(\vec{\theta})$ for any normalized trial state $|\psi(\vec{\theta})\rangle$ is always an upper bound to the true ground-state energy E_0:

$$E(\vec{\theta}) = \langle\psi(\vec{\theta})|\,\hat{H}\,|\psi(\vec{\theta})\rangle \quad \geq \quad E_0.$$

Because $E(\vec{\theta})$ depends on a set of parameters $\vec{\theta}$, the VQE iteratively updates these parameters to minimize the resultant energy. Once no further reduction in $E(\vec{\theta})$ is possible, the algorithm identifies that we reached the best approximation of E_0.

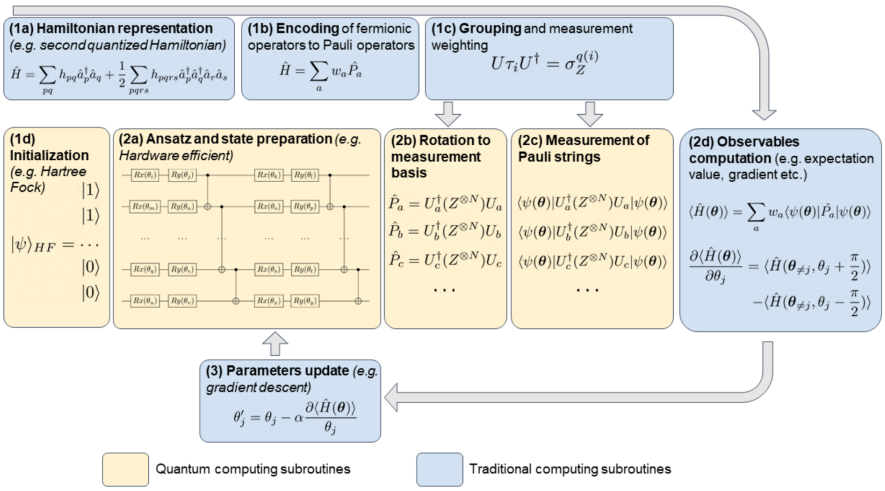

Figure 2.2: *VQE pipline[21].*

In this image, we find a flowchart of a VQE algorithm. Below, we describe the steps of the algoritm:

1. **Hamiltonian Construction and representation:** The first step of the algorithm is define the sytem for which we want to calculate the ground state. For that, we construc the Hamiltonian of the system. Constructing the Hamiltonian involves finding specific operators with their own weights.
2. **Encoding of operators:** The next step, is to encode Hamiltonian operators, on quantum computers, we can only measure observables expressed in Pauli basis, due to the two-lavel nature of qubits. In first quantization, the operators can be directly translated into spin operators. In second quantization, the operators are expressed as a linear combination of fermionic operators.
3. **Measurement of the Expected Energy:** The expectation value $\langle \psi(\vec{\theta}) \mid \hat{H} \mid \psi(\vec{\theta}) \rangle$ is obtained by measuring the appropriate Pauli operators on the quantum device, typically requiring multiple circuit executions due to non-commuting terms.
4. **Ansatz and State Preparation:** Once we have prepared the Hamiltonian such that we can measure his expectation value on a quantum device, we can proceed to the preparation of the wavefunction. To achieve this, we need to decide the parametrized quantum circuit, denoted as ansatz. One of the main aspects that we have to take into account, is that the ansatz must be sufficiently expressive to guarantee that it can appropriately aproximate the ground state wavefunction.
5. **Parameter Optimization:** Finally, the parameters of the ansatz used need to be updated iteratively until convergance. The measured energy serves as a cost function, we repeat the process until the convergence criteria is achieved.

   We can define the convergence criteria as:

   $$\left| E\left(\vec{\theta}_{k+1}\right) - E\left(\vec{\theta}_k\right) \right| < \delta,$$

   where δ is a small threshold for energy differences. The final set $\vec{\theta}^*$ yields an approximate ground-state wavefunction and energy.

2.4.2 Advantages and Challenges

VQE has garnered extensive interest in fields like **quantum chemistry**, **materials science**, and even combinatorial optimization problems mapped to Hamiltonians. Its hybrid structure allows leveraging near-term quantum devices (with limited qubits and gate depths) while offloading resource-intensive tasks—such as parameter updates—to classical computers.

Despite its promise, VQE faces several practical challenges:

- **Noise and Decoherence:** Real quantum devices suffer from errors that deteriorate the fidelity of prepared states and measurements, requiring error-mitigation strategies and noise-aware ansatz designs.
- **Barren Plateaus:** High-dimensional parameter spaces can contain large regions where gradients vanish, complicating the search for global minima.

- **Measurement Overhead:** Decomposing a Hamiltonian into many Pauli terms demands running multiple circuits, increasing sampling time and exposure to hardware noise.
- **Circuit Depth:** Accurate ansätze for complex systems may require deep circuits that quickly exceed the coherence times of current quantum processors.

2.4.3 Outlook in Quantum Simulation

Continuous improvements in hardware (qubit quality, gate fidelity, and error-correction schemes) and software (advanced ansätze, better optimizers, error mitigation) keep driving VQE toward practical applications. Recent strategies such as *ADAPT-VQE*[6], which determines a quasi-optimal ansatz with the minimal number of operators necessary to achieve the desired accuracy. The key idea is to systematically add fermionic operators oneatatime, such that the maximal amount of correlation energy is captured at each step.

As the number of qubits grows and quantum hardware evolves, VQE is likely to become a central approach for tackling classically intractable problems in quantum chemistry, materials science, and beyond. Its flexible hybrid nature will continue to serve as a testbed for new optimization algorithms, ansatz designs, and measurement strategies, bridging current *Noisy Intermediate-Scale Quantum (NISQ)* devices with the longer-term ambition of fault-tolerant quantum computing.

2.5 Ansätze

In the context of variational quantum algorithms and quantum chemistry, an **ansatz** is a carefully chosen, often physically motivated, parametric form of the quantum state used to approximate the ground state of a system described by a given Hamiltonian. The term *ansatz* originates from the German word “approach” or “initial guess,” and it reflects the central idea that we propose a functional form for the wavefunction and then we optimize the parameters in search of the lowest possible energy.

Within the framework of the Variational Quantum Eigensolver (VQE), the ansatz is implemented as a parameterized quantum circuit whose gates depend on a set of continuous variables $\vec{\theta}$. It is used to produce the trial state, with which the Hamiltonian can be measured to obtain an estimate energy, $E(\vec{\theta})$, which is then iteratively minimized by a classical optimizer. The key aspects of the ansatz are the expressiveness and trainability of the chosen ansatz. The expressibility is the ability of the ansatz to span a large class of states, while the trainability describes the practical ability of the ansatz to be optimized using techniques tractable on quantum devices in the Hilbert space.

Several ansätze have been proposed to achieve a balance between accuracy and computational cost. Below, we summarize the most relevant approaches, highlighting their theoretical underpinnings and current usage in quantum simulation[21].

2.5.1 Hartree–Fock-based Ansätze (Classical Reference)

A historically important "classical" ansatz in quantum chemistry arises from the **Hartree–Fock (HF)**[9] approximation. In this method, the total wavefunction is assumed to be a single Slater determinant constructed from one-particle orbitals. Although it captures the fundamental antisymmetry required by the Pauli exclusion principle, it neglects most of the electron correlation. Post-HF methods, such as Configuration Interaction (CI), Many-Body Perturbation Theory (MPn), and Coupled Cluster (CC), then build on this reference state by introducing additional terms that account for electron correlation.[15]

- **Configuration Interaction (CI):** Expands the wavefunction in a basis of Slater determinants (excitations) beyond the HF reference. The Full CI approach is exact within the chosen basis but scales exponentially with system size. Truncated CI methods (CIS, CID, CISD, etc.) reduce the computational cost but still grow quickly with system size.
- **Coupled Cluster (CC):** CC is a post Hartree-Fock method that aims at recovering a portion of electron correlation energy by evolving an initial wave function (usually the Hartree-Fock wave function) under the action of parametrized excitation operators. Formally written as

  $$|\Psi_{\mathrm{CC}}\rangle = e^{\hat{T}}|\Phi_{\mathrm{HF}}\rangle,$$

  where $\hat{T}$ is the sum of cluster excitation operators (singles, doubles, triples, etc.). Although Coupled Cluster with Singles and Doubles (CCSD) is often accurate, further inclusion of triples and higher excitations can be required for strongly correlated systems.

In the context of classical methods, these **ansätze** serve as trial wavefunctions whose coefficients are optimized using high-performance classical algorithms. Their conceptual basis—constructing physically motivated trial states that capture crucial features of the system—carries over into quantum computing.

2.5.2 Unitary Coupled Cluster (UCC)

A key adaptation of the Coupled Cluster theory to quantum computing is the **Unitary Coupled Cluster (UCC)** ansatz. It modifies the standard CC exponential by making it explicitly unitary:

$$|\Psi_{\mathrm{UCC}}\rangle = e^{\hat{T}(\vec{\theta})-\hat{T}^{\dagger}(\vec{\theta})}\,|\Phi_{\mathrm{HF}}\rangle,$$

where $\hat{T}(\vec{\theta})$ is typically truncated to include only single and double excitations (UCCSD). This approach guarantees that the resulting operator is unitary, which is crucial for hardware implementations in quantum computing since all gates must be unitary transformations.

- **UCCSD (Singles and Doubles):** The most widespread version of UCC is truncated at single and double excitations:

$$\hat{T}(\vec{\theta}) = \sum_{i,a} \theta_i^a \hat{a}_a^\dagger \hat{a}_i \; + \sum_{i,j,a,b} \theta_{i,j}^{a,b} \hat{a}_a^\dagger \hat{a}_b^\dagger \hat{a}_j \hat{a}_i \; + \cdots$$

  Here, i, j denote occupied orbitals and a, b virtual (unoccupied) orbitals. By exponentiating both $\hat{T}$ and $\hat{T}^\dagger$, the wavefunction stays normalized. However, the circuit depth can become large since implementing the exponential of a sum of non-commuting operators requires a trotterization or related approximation.

- **ADAPT-VQE and Variants:** To mitigate the high circuit cost, variants like *ADAPT-VQE* build up a UCC-type ansatz incrementally, selecting only those excitation operators that most significantly lower the energy at each step. This adaptive approach reduces the number of gates needed and often converges faster.

2.6 Optimizers

In quantum simulation algorithms such as the Variational Quantum Eigensolver (VQE), optimizers constitute a key element of the hybrid quantum-classical workflow. Their primary objective is to minimize the cost function

$$E(\vec{\theta}) = \langle \psi(\vec{\theta}) \mid \hat{H} \mid \psi(\vec{\theta}) \rangle,$$

where $\hat{H}$ represents the Hamiltonian of the system under study and $|\psi(\vec{\theta})\rangle$ is a parameterized quantum state, often referred to as the *ansatz*. After each quantum measurement, the optimizer updates the parameter vector $\vec{\theta}$ to guide the system toward the ground-state energy. This process is iterated until convergence, balancing the capabilities of quantum hardware with classical numerical techniques.

In the following subsections, we are going to describe, all the optimizers used in this project. While all these optimizers share the goal of efficiently navigating the parameter space, they differ in how they incorporate gradients, memory of past iterations, and adjustments of the learning rate.[17]

2.6.1 Gradient Descent (GD)

Gradient Descent is one of the most fundamental methods for continuous optimization. At each iteration, it updates parameters by moving them in the direction opposite to the gradient of the cost function:

$$\vec{\theta}_{k+1} = \vec{\theta}_k - \eta \nabla_{\vec{\theta}} E(\vec{\theta}_k),$$

where η is the learning rate and $\nabla_{\vec{\theta}} E(\vec{\theta})$ denotes the gradient of the cost function with respect to the parameters. Gradient Descent can converge slowly or get trapped in local minima when dealing with complex or high-dimensional landscapes, making it less efficient if used alone in large-scale molecular simulations.

2.6.2 Momentum Optimizer

The *Momentum* method extends standard Gradient Descent by incorporating a velocity term that accumulates a fraction of previous updates. This approach can mitigate oscillations and speed up convergence in regions with shallow gradients. The update rule is given by:

$$\vec{v}_{k+1} = \gamma \vec{v}_k + \eta \nabla_{\vec{\theta}} E(\vec{\theta}_k),$$
$$\vec{\theta}_{k+1} = \vec{\theta}_k - \vec{v}_{k+1},$$

where γ (typically between 0.9 and 0.99) is the momentum coefficient that controls how much past gradients influence the current update. This optimizer often accelerates learning in practice by effectively smoothing noisy or rapidly changing gradients.

2.6.3 Nesterov Momentum Optimizer (NMomentum)

Nesterov Momentum, sometimes referred to as *Nesterov's Accelerated Gradient (NAG)*, refines the idea of Momentum by anticipating the next position of the parameters before computing the gradient. Concretely, one computes the gradient at $\vec{\theta} + \gamma \vec{v}$ rather than at $\vec{\theta}$ only. The updates become:

$$\vec{v}_{k+1} = \gamma \vec{v}_k + \eta \nabla_{\vec{\theta}} E\big(\vec{\theta}_k + \gamma \vec{v}_k\big),$$
$$\vec{\theta}_{k+1} = \vec{\theta}_k - \vec{v}_{k+1}.$$

By 'looking ahead' in the direction of the velocity term, Nesterov Momentum tends to achieve smoother convergence and better performance on problems with numerous local minima or saddle points, which are common in complex quantum simulations.

2.6.4 RMSProp

RMSProp is a gradient-based optimizer that adaptively tunes the learning rate for each parameter by normalizing the gradient through a moving average of its recent magnitudes. This helps address issues of vanishing or exploding gradients, which can be particularly troublesome in variational circuits of moderate or large depth. Its core update equations are:

$$E[\nabla^2_{\vec{\theta}}]_k = \beta\, E[\nabla^2_{\vec{\theta}}]_{k-1} + (1-\beta)\, \nabla_{\vec{\theta}} E(\vec{\theta}_k)^2,$$
$$\vec{\theta}_{k+1} = \vec{\theta}_k - \eta \frac{\nabla_{\vec{\theta}} E(\vec{\theta}_k)}{\sqrt{E[\nabla^2_{\vec{\theta}}]_k + \epsilon}},$$

where $0 < \beta < 1$ is a decay factor controlling the smoothing effect, and ϵ is a small constant ensuring numerical stability.

2.6.5 Adagrad

Adagrad is an early approach to adaptive learning rates, designed to handle sparse or highly nonuniform gradients. It individually scales the updates by the inverse square

root of the cumulative sum of gradients:

$$\vec{\theta}_{k+1} = \vec{\theta}_k - \frac{\eta}{\sqrt{\sum_{i=1}^{k} \nabla_{\vec{\theta}} E(\vec{\theta}_i)^2} + \epsilon} \nabla_{\vec{\theta}} E(\vec{\theta}_k).$$

This mechanism allows parameters with small but consistent gradients to receive larger updates, which can be helpful in certain quantum chemistry models where specific Hamiltonian terms dominate.

2.6.6 Adam

Adam (Adaptive Moment Estimation) has emerged as one of the most widely used optimizers in machine learning and, increasingly, in quantum algorithms. It combines Momentum-like accumulations of the first moment of gradients (i.e., the mean) with an RMSProp-like treatment of the second moment (i.e., the uncentered variance). The update rules are:

$$\begin{aligned}
\vec{m}_{k+1} &= \beta_1 \vec{m}_k + (1-\beta_1) \nabla_{\vec{\theta}} E(\vec{\theta}_k), \\
\vec{v}_{k+1} &= \beta_2 \vec{v}_k + (1-\beta_2) \nabla_{\vec{\theta}} E(\vec{\theta}_k)^2, \\
\hat{\vec{m}}_{k+1} &= \frac{\vec{m}_{k+1}}{1-\beta_1^{k+1}}, \quad \hat{\vec{v}}_{k+1} = \frac{\vec{v}_{k+1}}{1-\beta_2^{k+1}}, \\
\vec{\theta}_{k+1} &= \vec{\theta}_k - \eta \frac{\hat{\vec{m}}_{k+1}}{\sqrt{\hat{\vec{v}}_{k+1}} + \epsilon},
\end{aligned}$$

where $0 < \beta_1, \beta_2 < 1$ are decay hyperparameters controlling how quickly the estimates of the first and second moments adjust. Adam's blend of adaptive step sizes and momentum often yields robust performance, even when the cost landscape is noisy or irregular, as is typical in quantum simulations.

2.6.7 Quantum Natural Gradient (QNG)

Unlike classical optimizers that rely on Euclidean metrics in parameter space, *Quantum Natural Gradient (QNG)* specifically incorporates the *Fubini–Study* metric, capturing how small changes in the parameters affect the underlying quantum state. This method is described in many *Penny Lane* resources. We can also find the theoretical foundations of this optimizer.[3] Conceptually, the update rule can be written as:

$$\vec{\theta}_{k+1} = \vec{\theta}_k - \eta \, \mathcal{F}^{-1} \nabla_{\vec{\theta}} E(\vec{\theta}_k),$$

where $\mathcal{F}$ represents the *quantum Fisher information matrix*, a matrix encoding the local geometry of the parameterized state. Computing $\mathcal{F}$ can be more demanding than classical gradients, but for many quantum chemistry, the improved efficiency justifies this added cost.

2.6.8 Importance of Optimizers in Quantum Simulation

Optimizers bridge the gap between quantum hardware and classical processing by iteratively refining the variational parameters to minimize the expectation value of the Hamiltonian. They must contend with challenges specific to quantum simulation, such as measurement noise, limited qubit counts, and complex cost landscapes characterized by local minima and barren plateaus. Properly choosing and tuning the optimizer is paramount to achieving accurate, resource-efficient simulations. By harnessing the distinctive advantages of adaptive and momentum-based methods—as well as more specialized quantum-aware techniques like QNG—one can significantly improve the speed and reliability of variational algorithms, thereby pushing the capabilities of quantum simulation closer to practical applications in molecular modeling.

CHAPTER 3

Methodology / project development

This chapter details the methodology used to execute the project, providing a clear and concise description of the approaches and techniques implemented to ensure replicability and academic rigor. It not only covers the research methods and measurement techniques but also delves into specific aspects of software development and project structuring. Whether the project involves computational modeling, algorithm implementation and software optimization, this section explains how each component contributes to the overall objectives.

Additionally, the chapter provides justifications for selecting specific methods over alternatives. For instance, the **PennyLane** framework was chosen over **Qiskit** for quantum simulations due to its robust documentation and practical examples in molecular simulations. The adoption of the **Variational Quantum Eigensolver (VQE)** algorithm was motivated by its compatibility with Noisy Intermediate-Scale Quantum (NISQ) devices. Parallelization strategies were implemented to enhance computational efficiency and reduce execution times.

The project follows a modular structure that facilitates scalability and simplifies the integration of new functionalities. The codebase is organized into configuration files, main execution scripts, and core computational modules. Furthermore, the adaptive construction of the *ansatz* and operator selection processes are described, highlighting how these techniques improve the accuracy and efficiency of quantum simulations.

Finally, the chapter addresses the limitations of the chosen methodologies and the strategies applied to mitigate these challenges. These include managing framework stability issues, computational resource constraints, and optimization convergence difficulties. By transparently discussing the strengths and weaknesses, this section presents a balanced view of the development process, emphasizing its reliability and robustness.

3.1 Tools and Frameworks Selection

To achieve the objectives of our project, the first essential step was to select the framework to be used throughout the development process. This decision was essential, as it directly influenced the progress and success of the project.

To make the decision on which framework to use, we compared the documentation of the two quantum simulation frameworks available in the market: *PennyLane* and *Qiskit*. These are the most comprehensive frameworks with similar features available at the time of creating this project. After reviewing the documentation, we ultimately chose to use *PennyLane* for two reasons.

The first reason was the amount of documentation related to quantum simulation. Once we started looking into how others were using these resources, we realized that in the field of molecular simulation, the existing documentation—both theoretical and especially practical—was substantially greater. This provided us with more examples to begin developing our project and a more extensive theoretical background to understand the concepts we were working with.

The second reason for our choice was the frequent major changes implemented by *Qiskit*. We realized that while *Qiskit* is a tool that promises to be high capable, it has historically undergone significant structural changes. For these reasons, this project has been developed using the *PennyLane* framework.

3.2 Project Structuring

After selecting the interface and implementing the initial version of the code, we reorganized the project to achieve a more modular architecture. This revised organization not only makes it easier to add new functionalities but also ensures that the project can handle higher levels of complexity. Below, we present the layout of the project and the functionality of each directory and file.

3.2.1 Code Organization

```
                    quantum_simulation_project/
config/
     config_functions.py: Configuration functions for the project.
     molecules.json: JSON file containing molecular data.
main.py: The main entry point for the program.
modules/
     ansatz_preparer.py: Quantum ansatz preparation.
     hamiltonian_builder.py: Molecular Hamiltonian construction.
     molecule_manager.py: Molecular data management.
     opt_mol.py: End-to-end molecular optimization.
     optimizer.py: Optimization algorithms.
     visualizer.py: Visualization tools.
temp_results_autograd/
     energy_evolution.png: Graph of energy convergence.
     filtered_report_autograd.txt: Filtered results report.
     final_geometries_3D.png: Final 3D geometries.
     nuclear_coordinates.png: Nuclear coordinates visualization.
     output.txt: Program output log.
     profile_output_autograd.txt: Autograd profiling output.
test/: Directory for tests.
```

3.2.2 Main Directory

- `main.py`: Central entry point of the program. It initializes the process by selecting molecules, configuring the optimizer, and setting up the ansatz. It also manages the optimization workflow, handles result storage, and produces comprehensive reports. Profiling tools evaluate computational performance.

3.2.3 `config/` Directory

- `config_functions.py`: Handles project configuration. This includes loading molecular data, selecting optimization algorithms, and setting initial parameters such as ansatz type and convergence tolerance. The module also allows adding custom molecules and organizing saved results.
- `molecules.json`: A structured JSON file containing information about molecules, including atomic symbols, coordinates, charges, and spin multiplicities.

3.2.4 `modules/` Directory

Core computational logic resides here:

- `ansatz_preparer.py`: Implements quantum circuit construction (ansätze) for both

adaptive and traditional methods. Includes the UCCSD ansatz (single and double excitations) and hardware-efficient ansatzes featuring multiple circuit layers.

- `hamiltonian_builder.py`: Constructs the molecular Hamiltonian, a fundamental component of quantum simulations. Calculates Hartree-Fock reference states and can extract exact energy values from the Hamiltonian matrix.
- `molecule_manager.py`: Initializes molecules by processing atomic symbols, initial coordinates, and configuration parameters such as charge and multiplicity. Also computes important properties like the number of electrons and orbitals.
- `optimizer.py`: Contains optimization algorithms (e.g., Adam, QNG, RMSProp). Integrates parameter updates and nuclear coordinate adjustments in a unified optimization framework.
- `opt_mol.py`: Orchestrates the complete molecular optimization pipeline. Brings together Hamiltonian construction, molecule management, optimization routines, and result visualization.
- `visualizer.py`: Offers visualization tools for energy convergence and molecular geometries. Generates detailed graphical outputs in both linear and logarithmic scales.

3.2.5 `temp_results_autograd/` Directory

Contains intermediate results generated during simulations:

- `energy_evolution.png`: Graph of energy convergence over iterations.
- `nuclear_coordinates.png`: Visualization of nuclear coordinates during optimization.
- `filtered_report_autograd.txt`: Filtered report of relevant profiling metrics.
- `output.txt`: Primary output log of the program.

3.3 Implementation of the VQE

Before delving into how molecular energy optimization has been implemented, it is crucial to first detail the methodology employed for optimizing the system parameters. This process was conducted using the *Variational Quantum Eigensolver* (VQE), which was selected as the primary method to estimate the ground state energy of the quantum system under study.

The VQE algorithm integrates limited quantum processing, characterized by measurements and shallow quantum circuits, with classical optimization techniques. Its selection is grounded on the following justifications:

- **Suitability for NISQ devices:** VQE is particularly well-suited for noisy intermediate-scale quantum (NISQ) devices, as it requires circuits of relatively low depth.
- **Flexible Ansatz:** It allows the use of various adaptive variational ansätze that capture essential electronic correlations.
- **Direct coupling to classical optimizers:** The VQE cost function (the expected energy) can be minimized with a wide range of classical methods, making it easy to experiment with different optimizers.

The core principle of VQE is the variational theorem, which guarantees that the expected energy of the ansatz is always an upper bound to the true ground state energy. By optimizing the ansatz parameters, the algorithm progressively approaches the actual energy minimum. We have already explained the concept of VQE in the state of the art chapter; now we will explain how we have implemented it in our project and how we have integrated it.

Principle of VQE:
The VQE is based on the variational principle, which states that the expected energy of any approximate state $|\psi(\theta)\rangle$ is always greater than or equal to the real ground state energy E_0:

$$E(\theta) = \langle \psi(\theta)|H|\psi(\theta)\rangle \geq E_0$$

We have already discussed this concept, but it is necessary to emphasize it as it is the foundation of the entire algorithm. The idea is to find the parameters θ that minimize the expected energy, thereby approaching the real value of the ground state energy.

Next, we will explore the implementation of the VQE within our project, breaking down its key components. Each element plays a crucial role in ensuring the algorithm's accuracy and efficiency: the molecular Hamiltonian defines the energy landscape, the ansatz captures electronic correlations through parameterized quantum circuits and the cost function evaluates the expected energy, guiding the optimization. This section outlines how each of these components was designed and integrated to maximize performance and precision.

3.3.1 Hamiltonian Construction Process

1. **Definition of Molecular Geometry:**

   Initially, it is necessary to define the molecular geometry of the system to be studied. This information includes the atomic symbols and the initial coordinates of the nuclei. In our project, this data is stored in a JSON file, which is loaded and processed to initialize the molecule. However, custom molecules can also be added directly in the code.

This part of the code provides the user with the ability to select the molecule to be simulated, allowing them to choose between the predefined molecules in the JSON file or add a new one. The `from_user_input` function loads the molecular information and initializes it, preparing it for simulation.

2. **Hamiltonian Construction:**

   Once the molecular geometry is defined, the next step is to construct the system's Hamiltonian. This Hamiltonian represents the total energy of the system and is fundamental for quantum simulation. In our project, the Hamiltonian is constructed using the `build_hamiltonian` function, which transforms the electronic Hamiltonian from its second-quantized form into a qubit-based representation. This implementation is relatively straightforward as it relies on PennyLane's `molecular_hamiltonian` function, which generates the Hamiltonian from the atomic symbols, coordinates, and other system parameters.

Hamiltonian Build

```
1 def build_hamiltonian(x, symbols, charge=0, mult=1, basis_name='sto
      -3g'):
2     x = np.array(x)
3     coordinates = x.reshape(-1, 3)
4     hamiltonian, qubits = qml.qchem.molecular_hamiltonian(
5         symbols, coordinates, charge=charge, mult=mult, basis=
              basis_name
6     )
7     h_coeffs, h_ops = hamiltonian.terms()
8     h_coeffs = np.array(h_coeffs)
9     return qml.Hamiltonian(h_coeffs, h_ops)
```

Note: A basis set, such as `sto-3g`, is chosen to represent atomic orbitals. This predefined set of basis functions simplifies the simulation while retaining sufficient accuracy for many molecular systems.

Apart from transforming the electronic Hamiltonian, initially expressed in its second-quantized form, into a qubit-based representation suitable for quantum computation, this function also allows the inclusion of user-defined parameters, such as the net molecular charge and the spin multiplicity, providing flexibility to simulate a wide range of electronic states. This feature is particularly important for accurately representing systems with different charge states and spin configurations.

Furthermore, it optionally supports the definition of an active space, allowing the focus to be limited to the most relevant orbitals and electrons, thus optimizing resource usage without sacrificing significant accuracy.

3.3.2 Adaptive Ansatz Construction and Operator Selection

For the construction of the ansatz, we use the adaptive ansatz construction builds upon the conventional variational approach by strategically selecting only those excitations that offer the most significant energy reductions. Instead of starting from a large, fixed set of parameters, the algorithm begins with the Hartree-Fock state and incrementally introduces new excitations based on their calculated impact on lowering the system's energy. This methodology provides both theoretical and practical advantages in handling the complexity of the solution space.

The selection process begins with a predefined *operator pool*, consisting of single and double excitation operators relevant to the molecular system. At the start of the procedure, no variational parameters are assigned, and the system is initialized in the reference Hartree-Fock state. At each iteration, the algorithm evaluates the energy gradients associated with adding each operator from the pool.

The following outlines the main steps of the adaptive ansatz construction and operator selection process, all implemented on the `ansatz_preparer.py` file:

1. **Gradient Calculation:** For every candidate operator $\hat{O}_i$ in the pool, the partial derivative of the energy with respect to the parameter controlling $\hat{O}_i$ is computed. This step identifies how sensitive the energy is to introducing that particular excitation. In our project this functionality is implemented in the `compute_operator_gradients` function.

Gradient Calculation

```
def compute_operator_gradients(operator_pool, selected_excitations,
     params, hamiltonian, hf_state, dev, spin_orbitals, ansatz_type
    ="uccsd"):
    gradients = []
    for gate_wires in operator_pool:
        param_init_autograd = np.array(0.0, requires_grad=True)

        @qml.qnode(dev, interface="autograd")
        def circuit_with_gate(param):
            prepare_ansatz(params, hf_state, selected_excitations,
                spin_orbitals, ansatz_type=ansatz_type)
            if len(gate_wires) == 2:
                qml.SingleExcitation(param, wires=gate_wires)
            elif len(gate_wires) == 4:
                qml.DoubleExcitation(param, wires=gate_wires)
            return qml.expval(hamiltonian)

        grad_fn_autograd = qml.grad(circuit_with_gate, argnum=0)
        grad = grad_fn_autograd(param_init_autograd)
        gradients.append(np.abs(grad))
```

```
18
19      return gradients
```

2. **Operator Ranking and Filtering:** All candidate excitations are ranked according to the absolute value of their gradients. Operators that produce negligible energy changes are discarded, while those offering substantial decreases are selected for inclusion. The `select_operator` function implements this filtering process.

Operation Ranking

```
1  def select_operator(gradients, operator_pool, convergence):
2      if len(gradients) == 0 or np.all(np.isnan(gradients)):
3          return None, None
4
5      max_grad_index = np.argmax(gradients)
6      max_grad_value = gradients[max_grad_index]
7
8      if max_grad_value < convergence:
9          return None, None
10     selected_gate = operator_pool[max_grad_index]
11     return selected_gate, max_grad_value
```

3. **Incremental Ansatz Growth:** The selected operator(s) is then added to the ansatz. A new parameter is introduced and optimized, increasing the dimensionality of the parameter space. This targeted expansion ensures that each additional parameter contributes meaningfully to lowering the energy. The incremental ansatz is implemented as follows:

Operation Ranking

```
1  def prepare_ansatz_uccsd(params, hf_state, selected_excitations,
       spin_orbitals):
2      qml.BasisState(hf_state, wires=range(spin_orbitals))
3      for i, exc in enumerate(selected_excitations):
4          if len(exc) == 2:
5              qml.SingleExcitation(params[i], wires=exc)
6          elif len(exc) == 4:
7              qml.DoubleExcitation(params[i], wires=exc)
```

4. **Pool Update and Iteration:** After adding the chosen operators, the process repeats. The operator pool is re-examined at subsequent steps, but it now excludes previously chosen operators unless they are included as parameterized parts of the ansatz. Over multiple iterations, the ansatz evolves adaptively, selecting the most

relevant subset of excitations.

Below, we can observe a simplified code snippet, consistent with the project's implementation, showcasing the adaptive operator selection process:

Adaptive Operator Selection

```
gradients = compute_operator_gradients(operator_pool,
    selected_excitations, params, hamiltonian, hf_state, dev,
    spin_orbitals)
selected_gate, max_grad_value = select_operator(gradients, operator_pool,
     convergence_threshold)
if selected_gate:
    selected_excitations.append(selected_gate)
    params = np.append(params, 0.0)  # Add new parameter for the chosen
        operator
    print(f"Added operator {selected_gate} with gradient {max_grad_value
        :.5e}")
else:
    print("No significant operators found. Convergence or local minimum
        reached.")
```

Adaptive Ansatz Benefits

In summary, this code uses the `compute_operator_gradients` function to evaluate each operator's gradient, while the `select_operator` function applies a filtering criterion based on a defined `convergence_threshold`. Only the most promising excitation is incorporated into the ansatz at each step, ensuring a controlled and meaningful expansion of the parameter space.

In numerical experiments, this targeted approach has demonstrated:

- **Faster Convergence:** Fewer parameters are introduced at each stage, allowing the optimizer to quickly reduce the energy without wading through irrelevant configurations.
- **Lower Resource Consumption:** By refining the search space, the quantum circuits remain relatively shallow, and classical optimization routines require fewer evaluations.
- **Scalability:** As molecular systems grow in complexity, the adaptive approach helps mitigate the exponential growth in parameter number, making it more feasible to handle larger systems within similar computational budgets.

3.3.3 Cost Function Definition

With the ansatz defined, the next step is to establish a cost function that evaluates the expected energy of the system given a set of parameters θ. In our implementation, this cost function is defined within `update_parameters_and_coordinates` and calculates the expected value of the molecular Hamiltonian:

Definition of the Cost Function

```
@qml.qnode(dev, interface=interface)
def cost_fn(params):
    prepare_ansatz(params, hf_state, selected_excitations, spin_orbitals)
    return qml.expval(hamiltonian)
```

In our implementation, `prepare_ansatz` serves as an auxiliary function that enables the selection of the desired ansatz for implementation. This flexibility has also allowed us to compare the effectiveness of the UCCSD ansatz against other ansätze. Below is the function that facilitates the selection of the ansatz to be used:

Ansatz Selection

```
def prepare_ansatz(params, hf_state, selected_excitations, spin_orbitals,
     ansatz_type="uccsd", num_layers = 10):
    if ansatz_type not in ANSATZ_MAP:
        raise ValueError(f"Ansatz type '{ansatz_type}' is not recognized.
             Available: {list(ANSATZ_MAP.keys())}")

    ansatz_fn = ANSATZ_MAP[ansatz_type]

    if ansatz_type == "uccsd":
        ansatz_fn(params, hf_state, selected_excitations, spin_orbitals)
    else:
        ansatz_fn(num_layers,params, hf_state, [], spin_orbitals)
```

This function is essential for evaluating $E(\theta)$. By calculating the expected value of the Hamiltonian, we can quantify how close our approximate state is to the true ground state.

3.4 Mixed Optimization Strategy

In this work, both the variational parameters θ (electronic) and the nuclear coordinates $\mathbf{X}$ (geometric) are refined within a single iterative loop. This coupled approach ensures that each electronic update reflects the current molecular geometry, while each geometric update leverages the most accurate electronic wavefunction available. By jointly optimizing θ and $\mathbf{X}$, the algorithm can converge more efficiently to a physically meaningful

global minimum.

3.4.1 Rationale for a Coupled Scheme

Traditional sequential approaches often optimize electronic parameters at a fixed geometry, then update the geometry using the finalized electronic structure. Such a split workflow can lead to unnecessary iterations and less-precise intermediate results. Because the electronic distribution and the molecular geometry are inherently interdependent, we opt to update both simultaneously, thereby reducing computational overhead and converging more smoothly to the system's equilibrium configuration.

3.4.2 Iterative Optimization Steps

The key steps of the coupled optimization process, implemented in the *run_optimization_uccsd* function within the `optimizer.py` file, are described below:

1. **Initialization:** First, we define the initial geometry $\mathbf{X}_0$, variational parameters θ_0, and other required structures.

Initialization

```
import pennylane as qml
from pennylane import numpy as np

# In run_single_optimizer (lines near 290+ in the code):
params = np.array([], requires_grad=True)  # Starting with empty
    parameters
operator_pool_copy = operator_pool.copy()
selected_excitations = []
x = x_init.copy()  # Copy of the initial geometry

# Set up the environment for optimization:
exact_energy = compute_exact_energy(symbols, x_init, charge, mult,
    basis_name)
hf_state = generate_hf_state(electrons, spin_orbitals)
dev = qml.device("default.qubit", wires=spin_orbitals)
```

2. **Hamiltonian Recalculation:** Then, at each iteration, the molecular Hamiltonian is rebuilt for the current geometry $\mathbf{X}$. This step ensures that the energy evaluation remains accurate and up-to-date with the latest nuclear configuration on each optimization cycle.

Hamiltonian Recalculation

```
# In run_optimization_uccsd (lines near 124+):
for iteration in range(max_iterations):
    # Rebuild the Hamiltonian for the current geometry 'x'
    hamiltonian = build_hamiltonian(x, symbols, charge, mult,
        basis_name)

    # Additional iteration logic follows:
```

3. **Electronic Update via Operator Gradients:** The next step is to compute the energy gradient with respect to a pool of candidate excitation operators. We select the operator that yields the largest energy decrease and add it to the ansatz. This strategy expands the variational parameter space only in directions that significantly reduce the energy.

Electronic Update

```
# Same loop in run_optimization_uccsd:
gradients = compute_operator_gradients(
    operator_pool_copy,
    selected_excitations,
    params,
    hamiltonian,
    hf_state,
    dev,
    spin_orbitals,
    ansatz_type="uccsd"
)

selected_gate, max_grad_value = select_operator(gradients,
    operator_pool_copy, CONV)
if selected_gate is None:
    print("No operators selected. Stopping optimization for uccsd."
        )
    break

selected_excitations.append(selected_gate)
params = np.append(params, 0.0)  # Add a new variational parameter
params = np.array(params, requires_grad=True)
print(f"Added operator {selected_gate} with gradient {
    max_grad_value:.5e}")
```

4. **Geometric Update via Finite Differences:** On the same iteration, we update the geometry by numerically approximating $\nabla_{\mathbf{X}} E(\theta, \mathbf{X})$through small perturbations to

each coordinate. The geometry is then updated as follows:

$$\mathbf{X} \leftarrow \mathbf{X} \; - \; \alpha \, \nabla_{\mathbf{X}} E(\theta, \mathbf{X}),$$

where α is a suitably chosen learning rate. This technique avoids overly complex gradient calculations while remaining flexible and straightforward to implement.

Geometric Update

```
# In update_parameters_and_coordinates (lines near 59+):
grad_x = compute_nuclear_gradients(
    params, x, symbols, selected_excitations, dev,
    hf_state, spin_orbitals, interface, charge, mult, basis_name
)

# Apply the update:
x = x - learning_rate_x * grad_x
```

5. **Convergence Checks:** Then, we impose strict thresholds on both the change in total energy and the geometric displacements. Once these criteria are satisfied, the geometry is deemed optimized and stable, and the refinement process is terminated.

Convergence Checks

```
# In update_parameters_and_coordinates (lines near 52+):
energy = np.real(energy)
if check_convergence(energy, prev_energy, recent_diffs):
    print(f"Convergence reached updating parameters and coordinates
        : Energy difference < {CONV}")
    converged = True
    prev_energy = energy
    # Code returns early, finalizing this substep
```

6. **Visualization and Termination:** Finally, we track the evolution of energy and geometry at every iteration, providing immediate graphical feedback (e.g., energy vs. iteration plots). This step helps identify convergence, reveals unexpected behaviors early, and confirms when additional optimization no longer benefits the system.

Visualization and Termination

```
# Example of final printout and logging in run_optimization_uccsd:
print(f"Iteration {iteration + 1}, Energy = {current_energy:.8f} Ha
    , Max Gradient = {max_grad_value:.5e}")

# After all iterations or once convergence is reached:
```

```
print(f"Total optimization time (uccsd): {total_time:.2f} seconds")
print(f"Final energy with {optimizer_name} (autograd) = {
    final_energy:.8f} Ha")
print(f"Difference from exact (FCI) energy: {diff:.8e} Ha")

# Geometry and circuit details are saved or printed:
for i, atom in enumerate(symbols):
    atoms_coords.append([atom, final_x_np[3*i], final_x_np[3*i+1],
        final_x_np[3*i+2]])
print(tabulate(atoms_coords, headers=["Symbol", "x (A)", "y (A)", "
    z (A)"], floatfmt=".6f"))
```

3.4.3 Efficiency of the Coupled Strategy

By refining θ and $\mathbf{X}$ concurrently, each electronic update leverages a geometry already progressing toward equilibrium. Likewise, every geometric move reflects the latest improvements to the electronic wavefunction. This synergy minimizes redundant calculations and avoids suboptimal solutions, typically leading to faster, more stable convergence compared to the conventional, decoupled approach.

3.5 Parallelization of Executions

One of the main improvements implemented in the project to accelerate execution and provide greater flexibility in our simulations has been parallelization. To achieve this, it was necessary to adapt the code so that simulations could be executed concurrently. Below, the process followed to enable this functionality is detailed.

3.5.1 User Input Management and System Configuration

To allow the user to configure the different types of simulations, a configuration file was incorporated in the `config/` directory, named `config_functions.py`. This file defines variables that allow specifying, among other things, the type of molecule, the optimizer, and the *ansatz*:

User Input Management

```
parser = argparse.ArgumentParser(description='Quantum simulation of
    molecules using VQE.')
parser.add_argument('--molecule', type=str, nargs='+', help='Molecule(s)
    to simulate.')
parser.add_argument('--optimizer', type=str, nargs='+', help='Optimizers
    to use (Adam, Adagrad, etc.).')
```

```
parser.add_argument('--stepsize', type=float, nargs='+', default=[0.4], help='Optimizer step size(s).')
parser.add_argument('--ansatz', type=str, nargs='+', help='Ansatz to use (e.g. uccsd, vqe_classic).')
args = parser.parse_args()
```

Before starting each simulation, two key lists are constructed:

- One with the optimizers to be used for each execution.
- Another with the additional parameters (the type of *ansatz*, the number of layers, the number of optimizations, etc.).

The `build_optimizers` function automatically generates the optimizers and organizes these parameters:

Generation of optimizers

```
def build_optimizers(args, ansatz_list, optimizer_map, predefined_steps):
    optimizers, new_ans = {}, []
    if args.all_optimizers:
        all_opts = list(optimizer_map.keys())
        user_steps = (args.stepsize != [0.4] or len(args.stepsize) > 1)
        for opt in all_opts:
            steps_for_opt = args.stepsize if user_steps else [predefined_steps[opt]]
            for step in steps_for_opt:
                for n in args.opt_step:
                    for ans_type, layer in ansatz_list:
                        name = f"{opt}_{step}_{ans_type}_{layer}layers_{n}steps"
                        optimizers[name] = optimizer_map[opt](stepsize=step)
                        new_ans.append((ans_type, layer, n))
    elif args.optimizer:
        for opt in args.optimizer:
            if opt not in optimizer_map:
                print(f"Error: Optimizer '{opt}' not recognized.")
                sys.exit(1)
            for step in args.stepsize:
                for n in args.opt_step:
                    for ans_type, layer in ansatz_list:
                        name = f"{opt}_{step}_{ans_type}_{layer}layers_{n}steps"
                        optimizers[name] = optimizer_map[opt](stepsize=step)
```

```
24                          new_ans.append((ans_type, layer, n))
25     else:
26         # Default value if neither --optimizer nor --all_optimizers is
               specified
27         for step in args.stepsize:
28             for n in args.opt_step:
29                 for ans_type, layer in ansatz_list:
30                     name = f"NMomentum_{step}_{ans_type}_{layer}layers_{n
                           }steps"
31                     optimizers[name] = NesterovMomentumOptimizer(stepsize
                           =step)
32                     new_ans.append((ans_type, layer, n))
33     return optimizers, new_ans
```

3.5.2 Parallelization of Execution with Multiple Optimizers

After generating the optimizers and their corresponding configurations, the parallel execution process is invoked. This approach distributes each simulation across different processes using `ProcessPoolExecutor`, thereby leveraging multiple CPU cores to significantly speed up computation time:

Process parallelization

```
1  with concurrent.futures.ProcessPoolExecutor() as executor:
2      futures = []
3      cont = 0
4      for optimizer_name, opt in optimizers.items():
5          if cont < len(ansatz_list):
6              ans_type, layers, nsteps = ansatz_list[cont]
7          else:
8              ans_type, layers, nsteps = ("uccsd", 0, 10)
9          cont += 1
10         futures.append(
11             executor.submit(
12                 run_single_optimizer,
13                 optimizer_name, opt, ans_type, layers, nsteps, symbols,
                       x_init, electrons, spin_orbitals, charge,
14                 mult, basis_name, hf_state, dev, operator_pool,
                       exact_energy, results_dir
15             )
16         )
```

In this way, each optimizer is executed independently, allowing for the maximum utilization of available hardware resources. This accelerates the simulation process and

provides greater flexibility in experimenting with different configurations.

3.5.3 Compilation of Results and Cleanup of Temporary Files

After completing the execution of parallel processes, several key steps are carried out to unify results, clean up temporary files, and generate the final results. Each step is detailed below along with the corresponding code.

Creation and Execution of Parallel Processes

Parallel processes are created using `ProcessPoolExecutor`. For each configured optimizer, simulations are submitted as tasks to the executor, and the corresponding *futures* are stored. Once they complete, the results are collected in the `interface_results` dictionary.

Creation and Execution of Parallel Processes

```
# Collect results when processes finish
for future in concurrent.futures.as_completed(futures):
    optimizer_name, data = future.result()
    interface_results[optimizer_name] = data
```

Unification of Results into a Single File

To centralize the simulation information, the contents of individual output files are combined into a single file named `combined_output.txt`.

Unification of Results into a Single File

```
combined_output_path = os.path.join(results_dir, "combined_output.txt")
with open(combined_output_path, "w", encoding="utf-8") as combined_out:
    for optimizer_name in optimizers.keys():
        output_file = os.path.join(results_dir, f"output_{optimizer_name
            }.txt")
        if os.path.exists(output_file):
            with open(output_file, "r", encoding="utf-8") as f:
                content = f.read()
            combined_out.write(f"=== Optimizer: {optimizer_name} ===\n")
            combined_out.write(content + "\n")
```

Deletion of Temporary Files

Once the individual data has been centralized, the temporary output files are deleted to reduce disk space usage and clean the results directory.

Deletion of Temporary Files

```
for optimizer_name in optimizers.keys():
    output_file = os.path.join(results_dir, f"output_{optimizer_name}.txt
        ")
    if os.path.exists(output_file):
        os.remove(output_file)
```

Generation of Final Results

The final results, such as the optimized energy, differences from the exact energy, and final molecular geometries, are presented to the user. Additionally, execution times and corresponding quantum circuits are visualized.

Generation of Final Results

```
print("=== Total Optimization Times ===\n")
for optimizer_name in optimizers.keys():
    final_energy = interface_results[optimizer_name]["final_energy"]
    exact_energy_ref = interface_results[optimizer_name]["
        exact_energy_reference"]
    diff = final_energy - exact_energy_ref if final_energy is not None
        else None
    if final_energy is not None:
        print(f"Final energy with {optimizer_name} = {final_energy:.8f}
            Ha")
        print(f"Difference from exact (FCI) energy: {diff:.8e} Ha\n")
    else:
        print(f"No final energy obtained with {optimizer_name}\n")

    total_time = interface_results[optimizer_name]["execution_times"].get
        ('Total Time', 0)
    print(f"Optimizer: {optimizer_name}, Time: {total_time:.2f} seconds")
```

In this way, the complete workflow allows:

1. Executing processes in parallel and collecting their results.
2. Unifying the generated data into a single output file.
3. Cleaning up temporary files to maintain an organized directory.
4. Presenting the final results in a clear and detailed manner.

CHAPTER 4

Results

This chapter should encompass your data analysis and findings. Additionally, include relevant tables, figures, and citations to support your results and interpretations. Here is a suggested list of topics to discuss:

4.1 Interface Comparison

During the development of this project, various experiments were conducted to optimize the performance of a quantum molecular simulator. In this context, the choice of the interface for calculating cost functions is crucial, as these functions must be optimized to obtain the optimal state and geometry of each molecule. Typically, the *JAX* interface is the most widely used due to its GPU acceleration capabilities, which generally provide greater efficiency and speed in searching for the minimum of the cost function.

However, when comparing two identical implementations—varying only the calculation interface—we observed an unexpected result: the *JAX*-based interfacerunning on a GPU was slower than the *autograd*-based interface on a CPU. To confirm that this was not a coding error, we repeated the experiments on different machines, obtaining the same result. For this reason, we opted to continue with the *autograd* interface due to its greater speed in our specific implementation.

4.1.1 Optimization and Timing Logging

To verify the performance differences between both interfaces, the same optimization was executed while varying only the interface. During these simulations, the execution times of the different functions in the code were recorded, with their values shown in Table 4.1.

Function	[Li, H] _autograd_GD	[Li, H] _jax_GD	[O, H, H] _autograd_GD	[O, H, H] _jax_GD	[H, H] _autograd_GD	[H, H] _jax_GD
Iteration 1	1246.7627	6251.3362	6942.21696	39003.89009	14.6908	40.5485
Iteration 2	1244.0321	6284.9812	6935.09353	40652.7751	14.7824	36.2979
Iteration 3	1247.4399	6348.2470	6920.68571	40386.29868	14.9931	38.6236
Iteration 4	1245.7256	6351.6437	6942.60873	40128.31419	15.0694	39.1362
Iteration 5	1244.8591	6349.5099	6965.70663	40657.74473	15.1512	40.6186
Total Time	6228.8195	31585.7475	34706.3116	200829.0866	74.6870	195.2551
build_hamiltonian	29.1349	30.3407	78.4744	85.7532	0.4934	0.5329
compute_operator_gradients	1533.0319	17497.4381	12563.3726	113792.7167	0.6313	11.9006
update_parameters_and_coordinates	4666.6385	14056.6795	22064.4153	86946.6021	73.5594	182.5271

Table 4.1: *Execution times for different molecules and interfaces using Gradient Descent.*

Figure 4.1 shows how the execution time evolves over the iterations for each molecule and type of interface. It is evident that, in all cases, the *autograd*-based interface offers lower computation times than the *JAX*-based interface.

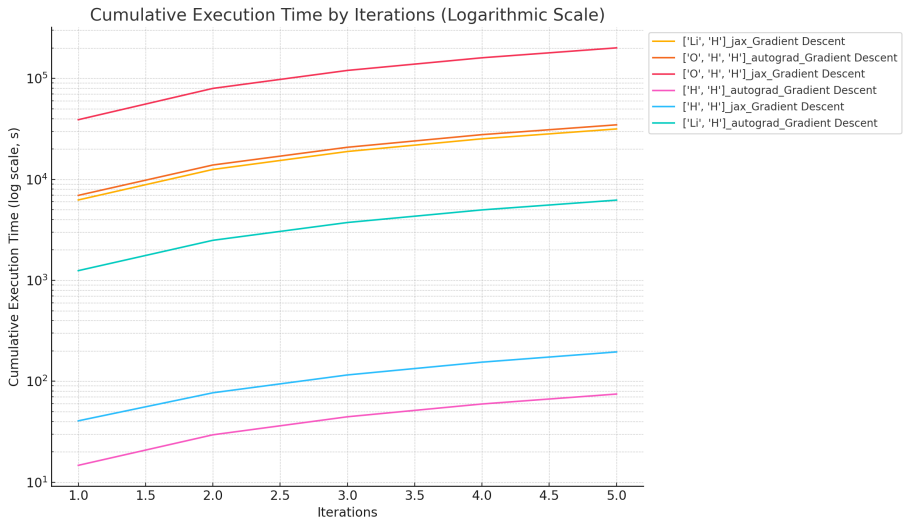

Figure 4.1: *Execution time of different molecules per iteration in the simulation.*

Comparative Performance Analysis

To evaluate the performance of both interfaces in more detail, a table was created showing the percentage increase in execution time of *JAX* compared to *autograd*, as seen in Table 4.2.

Metric	LiH	H_2	H_2O	Mean
Total Time	80.28%	82.72%	61.75%	74.92%
build_hamiltonian	3.97%	8.49%	7.42%	6.63%
compute_operator_gradients	91.24%	88.96%	94.70%	91.63%
update_parameters_and_coordinates	66.80%	74.62%	59.70%	67.04%

Table 4.2: *Comparison of execution times between JAX and autograd interfaces for different molecules.*

On average, it was observed that the *JAX* interface exhibits a 74.92% higher total execution time than the *autograd* interface. Additionally, it is interesting to note that as the complexity of the molecule increases (with a greater number of atoms), the penalty percentage of *JAX* tends to decrease. This behavior suggests that, in larger-scale problems, GPU acceleration could become more competitive, although it does not manage to outperform *autograd* in this implementation.

4.1.2 Computation Time per Function

For a higher level of detail, the computation time was also measured for each part of the code where the interface change is introduced. Figure 4.2 shows the accumulated execution times in the main stages of the algorithm.

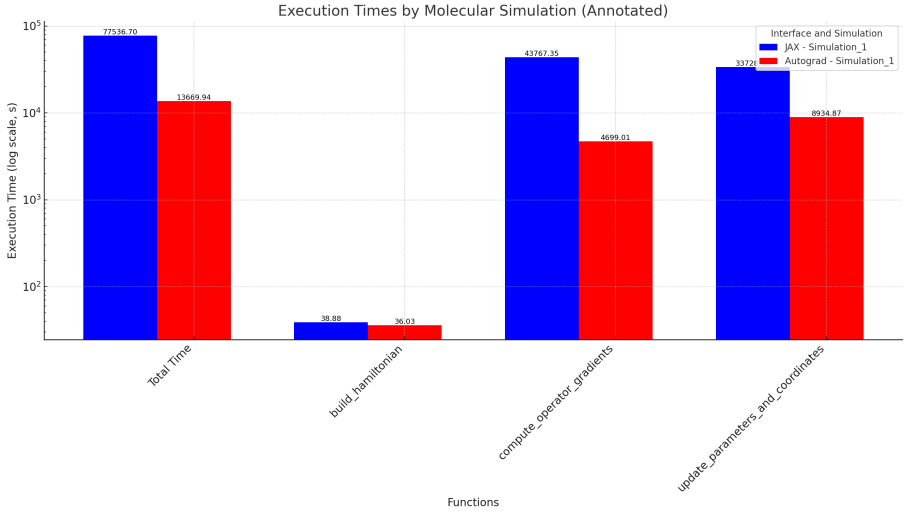

Figure 4.2: *Execution time in different parts of the code.*

The same pattern is maintained in all functions: the *JAX* interface records higher execution times than *autograd*. In particular, the gradient computation part `compute_operator_gradients`

increases its execution time by 91.68% when using *JAX*. This difference is largely attributed to the overhead caused by data transfer between the CPU and GPU, especially given that *PennyLane* does not fully support Hamiltonian generation on the GPU.

On the other hand, the function `update_parameters_and_coordinates`, responsible for performing the molecular geometry and parameter optimization step, also shows a 67.04% increase when using *JAX*. Nevertheless, it is worth highlighting that as the problem grows in complexity, the *JAX* interface gains some relative efficiency in gradient calculation; however, the time saved through GPU acceleration is offset by the continuous data transfer between CPU and GPU throughout the iterations.

4.1.3 Conclusions

Based on the obtained results, the *autograd* interface demonstrated superior performance in terms of speed for our implementation of the quantum molecular simulator. Although the GPU is usually advantageous in larger-scale problems, the data transfer overhead and the lack of full support for Hamiltonian generation within the GPU reduced the efficiency of *JAX*. For this reason, we ultimately chose to use the *autograd* interface for the final implementation of the quantum molecular simulator.

4.2 Ansatz Comparison

One of the most significant modifications affecting our code and its functionality has been the choice of the Ansatz. Our proposal has been to implement UCCSD, an Ansatz typically used for this type of simulation, as it enhances the simulation performance by achieving higher efficiency. The efficacy of this type of Ansatz has already been demonstrated, showing how it can improve simulation performance by producing more optimal quantum circuits without the need to create a specific Ansatz for the molecule being simulated. Indeed, for each optimizer configuration and for each different molecule simulation, there exists an optimal quantum circuit that achieves the best performance. However, since our objective is to develop a program that can simulate various molecules with maximum performance, we observe that the best option is UCCSD. To illustrate how our simulation performance is improved, we have generated Ansätze with different levels of depth and compared their performance with that of a UCCSD Ansatz. We have simulated various configurations of classical Ansätze, and in all cases, the UCCSD Ansatz has achieved better performance. More complex and molecule-specific Ansätze could be tested, but it is unlikely that another type of Ansatz would outperform UCCSD in terms of performance improvement.

Below is a simulation with different Ansatz depths and varying numbers of iterations obtained directly from the simulation.

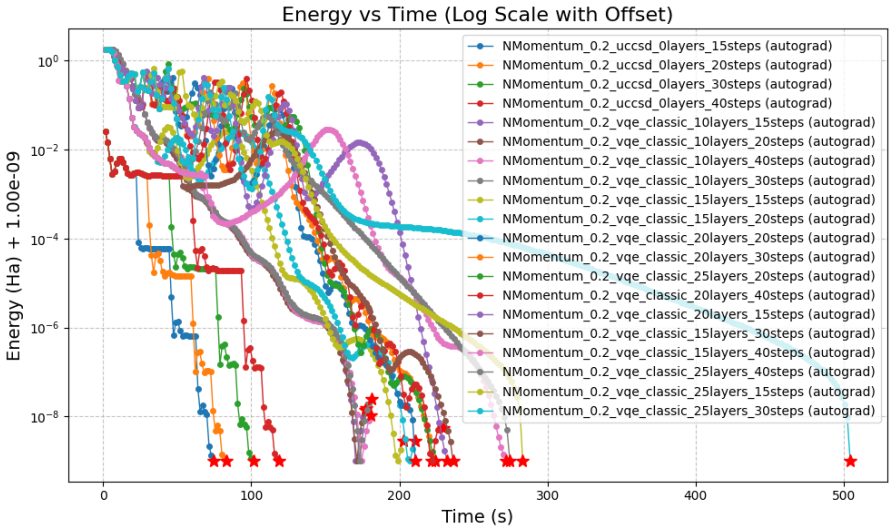

Figure 4.3: *Energy vs. Time for different Ansätze and iterations.*

It is observed that the UCCSD Ansatz achieves the best performance in all simulations, regardless of the number of optimizations performed for each iteration. For greater clarity of the results, a simulation was conducted with only a single number of optimizations per iteration, and the performance of the different Ansätze was compared, providing a clearer view of how UCCSD achieves the optimal performance.

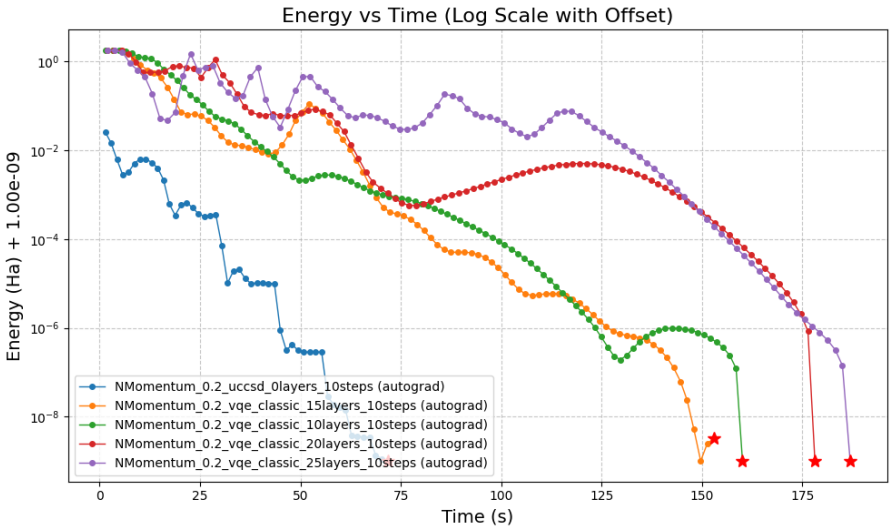

Figure 4.4: *Energy vs. Time for different Ansätze.*

Finally, to corroborate that the UCCSD Ansatz achieves the best performance, a simulation was conducted with a different molecule, and the performance of the various Ansätze was compared. In the following image, it can be seen that the UCCSD Ansatz achieves highest efficiency in all simulations.

4.3 Optimizer

Once the Ansatz was selected, the next step was to test the functionality of our project, and thus see how it could help us improve the performance of our simulations. For this purpose, a series of tests were carried out using the capabilities previously designed for performance improvement. The tests were performed with a single Ansatz, UCCSD, and for the following molecules: H2, LiH, and H2O.

The steps followed for the realization of the tests were as follows:

4.3.1 Optimizer Selection

The first step was to determine the optimizer for the different molecules. To achieve this, we developed a procedure that allowed executing the same molecules with various optimizers, each covering a range of *step size* values. This approach enabled the comparison of the different optimizers to be as fair as possible.

In the first phase, which executed 42 processes in parallel, observing which *step size* offered the best performance for each optimizer and molecule. Subsequently, the simulation was repeated using only those optimal *step sizes*, thereby achieving greater accuracy in the optimal *step size* value for each optimizer, which will be discussed in the next section. The results of this second simulation are presented below.

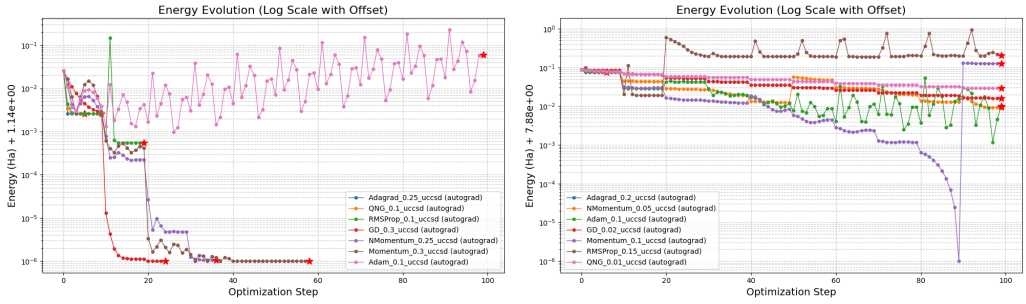

(a) *H2 simulation.* **(b)** *LiH simulation.*

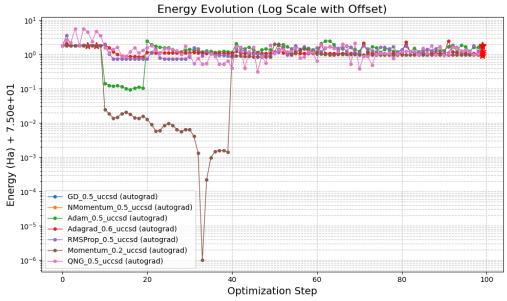

(c) *H2O simulation.*

Figure 4.5: *Optimal* step size *selection for each optimizer and molecule.*

To delve deeper into the performance of the different optimizers, the following tables

present the final energy, total optimization time, and the number of iterations required to converge for each molecule.

Table 4.3: *Final energy and optimization time for* H_2, LiH, *and* H_2O *using various optimizers.*

Molecule	Optimizer	Final Energy (Ha)	Total Time (s)	Iterations
H_2	Adam (0.1)	-1.07655292	173.30	10
	Adagrad (0.25)	-1.13469066	10.19	1
	NMomentum (0.25)	-1.13730600	62.84	4
	Momentum (0.3)	**−1.13730605**	100.43	6
	RMSProp (0.1)	-1.13675411	33.14	2
	GD (0.3)	**−1.13730605**	41.77	3
	QNG (0.1)	-1.13469066	18.40	1
LiH	Adam (0.1)	-7.87024707	13444.57	10
	Adagrad (0.2)	-7.80548501	977.86	1
	NMomentum (0.05)	**−7.87085783**	13442.59	10
	Momentum (0.1)	-7.75267240	13566.98	10
	RMSProp (0.15)	-7.67650000	13671.22	10
	GD (0.02)	-7.86422129	13449.49	10
	QNG (0.01)	-7.85120449	13776.00	10
H_2O	Adam (0.5)	-73.75990609	28454.49	10
	Adagrad (0.6)	-73.93046296	28891.08	10
	NMomentum (0.5)	-73.22152796	7497.83	1
	Momentum (0.2)	**−74.03997489**	68420.47	10
	RMSProp (0.5)	-73.28585876	65470.02	10
	GD (0.5)	-73.22152796	**6486.79**	1
	QNG (0.5)	-73.13971041	70716.22	10

In the evolution of the 3 iterations, we observed that the *Momentum* optimizer was the one that offered the best performance in all the molecules. In the case of LiH, it is observed that it converges best until it reaches a geometric optimization, at which point it fails to converge. This is because the *step size* is not yet fully optimized. Even so, we conclude that for the three simulations, the *Momentum* optimizer is the one that offers the best performance.

An optimizer that also offers good performance is *Adagrad.* Although it does not converge as effectively as *Momentum*, it provides great speed in the simulations.

4.3.2 Step Size Selection

To determine the most suitable *step size* range, we started with the optimal value identified during optimizer selection. Subsequently, additional simulations were designed with values close to the initial optimum to refine this selection.

This section presents the evolution of energy as a function of iterations, considering different *step size* values for each molecule.

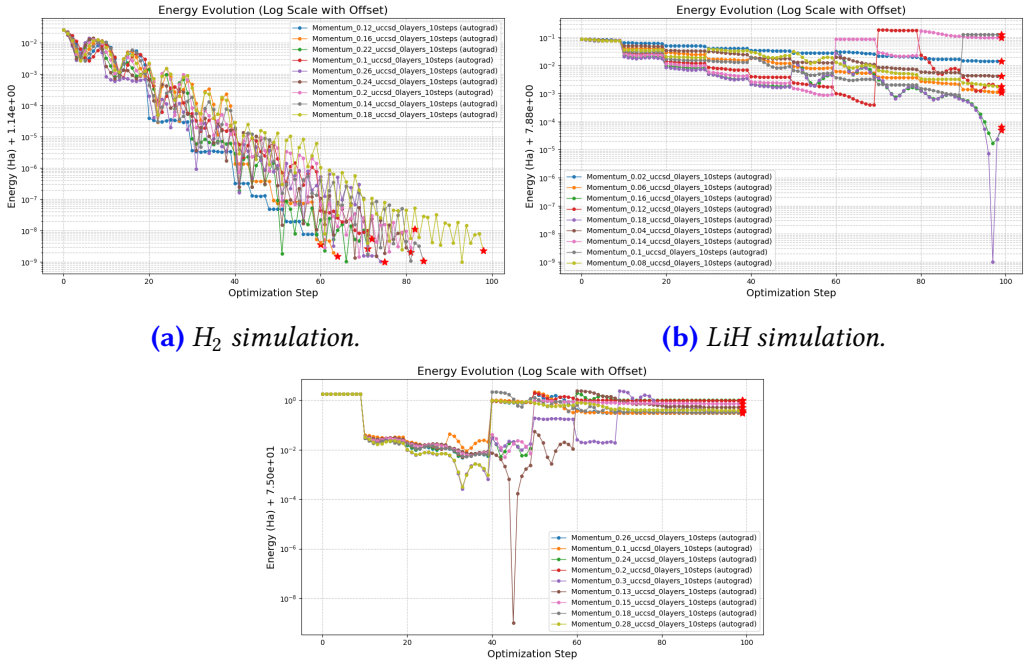

(a) *H_2 simulation.* **(b)** *LiH simulation.*

(c) *H_2O simulation.*

Figure 4.6: *Energy evolution as a function of step size for different molecules.*

Observing the graphs, we were able to see that for the molecules H_2 and LiH, the optimal *step size* was clear, being 0.12 and 0.16 respectively. However, it was observed that for the molecule H_2O, the optimal *step size* was not as clear, as there were several values that offered good performance.

For this reason, we created a table again to better observe the results. Note that in this case, each row corresponds to a *step size*, keeping the same optimizer (case, **Momentum**).

Table 4.4: *Final energy and optimization time for* H_2, LiH, *and* H_2O *varying the step size (optimizer: Momentum).*

Molecule	Step Size	Final Energy (Ha)	Total Time (s)	Iterations
LiH	0.02	-7.86678430	**13915.43**	10
	0.04	-7.87699744	14001.06	10
	0.06	-7.88014045	13916.11	10
	0.08	-7.87944832	14144.26	10
	0.10	-7.75267240	14098.79	10
	0.12	-7.87992395	13937.66	10
	0.14	-7.78203292	14063.16	10
	0.16	**−7.88118152**	13931.81	10
	0.18	-7.88116774	13998.38	10
H_2	0.10	**−1.13730605**	113.23	10
	0.12	**−1.13730605**	**92.55**	10
	0.14	**−1.13730605**	131.52	10
	0.16	**−1.13730605**	101.46	10
	0.18	**−1.13730605**	149.96	10
	0.20	-1.13730604	128.31	10
	0.22	**−1.13730605**	111.54	10
	0.24	**−1.13730605**	123.74	10
	0.26	**−1.13730605**	115.02	10
H_2O	0.10	**−74.68985518**	48577.15	10
	0.13	-74.46832273	74175.94	10
	0.15	-74.25355192	74211.21	10
	0.18	-74.67526296	75127.97	10
	0.20	-74.03997489	73130.72	10
	0.24	-73.99558215	56465.58	10
	0.26	-74.68963596	**44970.94**	10
	0.28	-74.59437540	75555.08	10
	0.30	-74.65314486	73575.44	10

Finally, thanks to the table, we were able to see that, for H_2O, the *step size* 0.10 was the one that gave the most optimal energy value, being slightly superior to 0.26.

Thus, we conclude that the optimal *step size* values for the *Momentum* optimizer are those found between 0.1 and 0.2, specifically, 0.12 for LiH, 0.12 for H_2, and 0.10 for H_2O.

4.3.3 Number of Subiterations

Finally, the last step that we performed to improve the performance of the simulation was in the number of subiterations that the optimization performs. By this, we refer to the iterations that are performed to optimize the parameters of each geometric position that we are optimizing the molecule. Since this is the process where most computational cost is incurred, it is a crucial step to improve the performance of the simulation.

To be able to configure in the most effective way the number of subiterations, we have generated a series of simulations with different numbers of subiterations, and we have

observed the evolution of the energy. The configuration of the optimizers has been with the optimal values that we have obtained from the previous tests, with the Momentum optimizer and the step size values optimal for each molecule. Finally, the results have been compared with the values obtained from the following database: NIST Computational Chemistry Comparison and Benchmark DataBase.

Below are the graphs obtained from the different simulations:

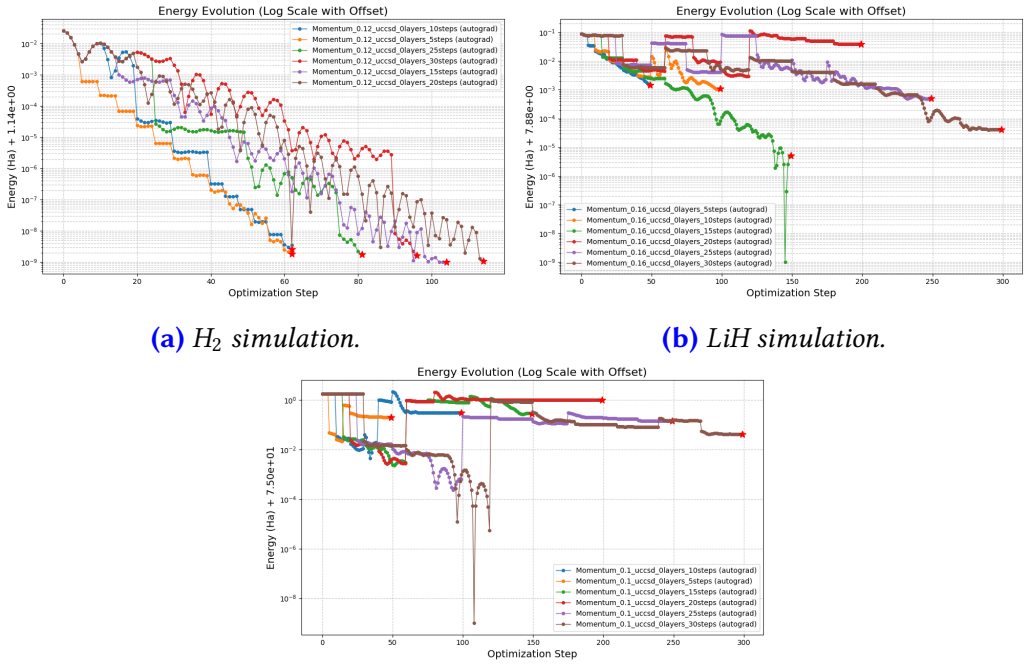

(a) *H_2 simulation.* **(b)** *LiH simulation.*

(c) *H_2O simulation.*

Figure 4.7: *Energy evolution as a function of number of iterations for different molecules.*

Initial Results

As in previous sections, to clarify the results, we have generated tables of the results that serve as tools for analyzing the outcomes in greater depth.

Table 4.5: *Final energy and optimization time for* H_2, LiH, *and* H_2O *using Momentum optimizer with varying steps.*

Molecule	Steps	Final Energy (Ha)	Total Time (s)	Difference from FCI (Ha)
H_2	5	**−1.13730605**	101.86	0.00000005
	10	**−1.13730605**	**99.08**	0.00000005
	15	**−1.13730605**	163.25	0.00000005
	20	**−1.13730605**	175.06	0.00000005
	25	**−1.13730605**	124.58	0.00000005
	30	**−1.13730605**	147.59	0.00000005
LiH	5	−7.88079149	**8328.30**	0.00174651
	10	−7.88118152	13365.38	**0.00135648**
	15	−7.88226478	18384.78	0.00027322
	20	−7.84260017	23309.87	0.03993783
	25	−7.88176386	28433.90	0.00077414
	30	**−7.88222895**	33421.15	**0.00030905**
H_2O	5	−74.79245495	**50836.87**	0.22251505
	10	−74.68985518	45559.48	0.32511482
	15	−74.70554258	77448.07	0.30942742
	20	−74.00851054	113172.24	1.00645946
	25	−74.84425344	136497.21	0.17071656
	30	**−74.94705746**	157949.56	**0.06791254**

We clearly observe that for the molecule H_2, the number of subiterations does not affect the final result. In this case, as it is such a basic molecule with few parameters, the simulation converges relatively easily for all configurations. Thus, we observe that the best option, due to its speed and accuracy, and yielding the best performance, is the configuration with 10 subiterations per geometric position, with an execution time of 99.08 seconds, being 2.72% faster than the configuration with 5 subiterations.

In the case of LiH, the energy −7.88222895 Ha achieved in 30 steps shows the best accuracy compared to the reference value. However, as we are interested in a balance between performance and accuracy, by observing the execution times and results, we find that the optimal performances are achieved with a number of subiterations between 5 and 10 per geometric optimization cycle. Considering that the accuracy with 10 subiterations is 22.33% higher but with a 37.68% increase in computation time, we conclude that the process with highest efficiency is that with 5 subiterations.

For the molecule H_2O, we find the same result as for the molecule LiH, where the highest accuracy is obtained with 30 subiterations, but the best performance is achieved with 5 to 10 subiterations per cycle. Making the same comparison as before, we find that with 10.38% less computation, we obtain 31.55% less accuracy, so the optimal performance is achieved with 5 subiterations.

The results show that highest efficiency is found between 5 and 10 subiterations per geometric optimization cycle, achieving a balance between accuracy and computation time. This leads us to conclude that the best option is 10 subiterations for the molecule

H_2, and 5 subiterations for the molecules LiH and H_2O. For this reason, we have decided to analyze how these molecules evolve with this number of subiterations. The results obtained are presented below.

Final phase

To find a more precise value for the optimal number of subiterations, we conducted the same simulations as in the previous sections, but varying the number of subiterations in our simulations, setting them to values from 2 to 10. This allowed us to observe more clearly how the hybrid optimization technique implemented in our project affects the results.

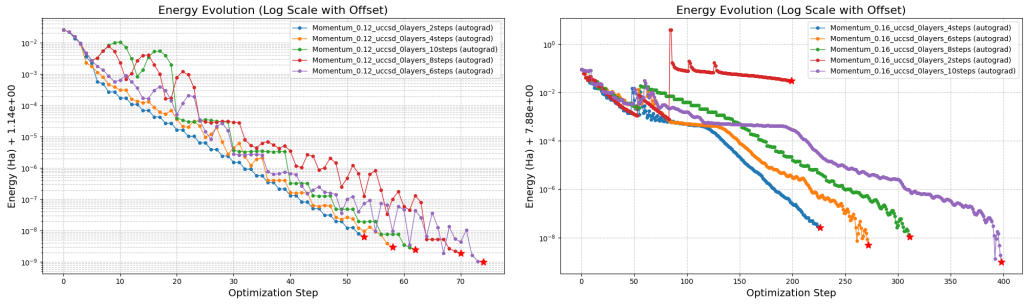

(a) *H_2 simulation.* **(b)** *LiH simulation.*

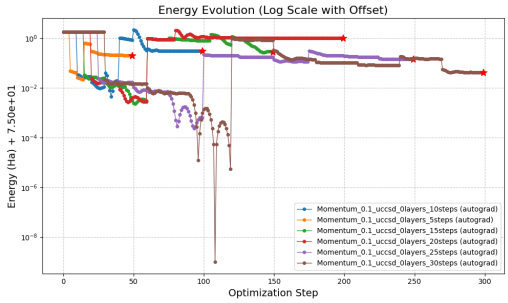

(c) *H_2O simulation.*

Figure 4.8: *Energy evolution as a function of number of iterations for different molecules.*

In the graphs obtained from this second simulation, the effect of hybrid optimization on convergence is clearly observed. The fewer the number of subiterations, the faster the convergence. However, this has a negative effect, as the optimization becomes more unstable and imprecise. We observe that in the molecule H_2, convergence is faster with 2 subiterations. In the case of LiH, the most effective simulation is with 4 subiterations. Additionally, it is observed that reducing to 2 subiterations causes the simulation to fail to converge due to the instability of the optimization. The data from both simulations are presented below.

Table 4.6: *Final energy and optimization time for* H_2 *and* LiH.

Molecule	Steps	Final Energy (Ha)	Total Time (s)	Difference from FCI (Ha)
H_2	2	−1.13730605	**95.57**	0.00000005
	4	−1.13730605	96.65	0.00000005
	6	−1.13730605	122.50	0.00000005
	8	−1.13730605	111.27	0.00000005
	10	−1.13730605	98.74	0.00000005
LiH	2	−7.85253665	51461.91	0.03000135
	4	**−7.88275270**	**40118.76**	**0.00021470**
	6	−7.88275272	40896.30	0.00021472
	8	−7.88275272	43240.40	0.00021472
	10	−7.88275272	43240.40	0.00021472

4.4 Limitations

During the tests conducted, we identified various limitations that may have affected the results. The most significant limitation has been the lack of implementation of quantum error simulations. In all simulations, the negative effects of errors that can occur in real quantum computers have not been considered. For this reason, we cannot assert that these same results would be useful for a similar implementation on a real quantum computer.

Similarly, we did not have access to a quantum computer, which would have been extremely helpful in validating the proper functionality of our project. Even so, we have been able to verify that our project performs optimally and that the implementation of hybrid optimization is effective in improving the performance of the simulations.

Another limiting aspect has been the computational capacity of our computer. Since we do not have access to a quantum computer, simulations with a high number of molecules have been very costly in terms of computational time.

CHAPTER 5

Sustainability Analysis and Ethical Implications

5.1 Sustainability Matrix

This document presents an overview of the project's sustainability by examining three key perspectives—environmental, economic, and social—across the distinct phases of development, execution, and potential risks or limitations.

5.1.1 Environmental Perspective

Development

The development phase of the project required approximately 540 hours of work. To carry out this work, I used a Mac laptop with an average power consumption of 30 W and a high-performance computing (HPC) server provided by a Viennese research center. This server, equipped with 16 CPU threads, operates at around 200 W under heavy workloads. Combining these resources allowed me to optimize performance while avoiding additional hardware acquisition or excessive energy consumption.

Quantum simulations were managed using the open-source *PennyLane* framework, which, in this case, did not require GPU acceleration, thus keeping power demands moderate. Additionally, I minimized environmental impact during commuting by traveling approximately 3.5 km per day via metro over 120 days. Factoring in all these contributions, the total emissions for the project are estimated to be 32.73 kg of CO_2. While I did not explicitly follow a circular economy model, I prioritized reusing existing infrastructure and avoided purchasing new devices, which further reduced potential waste.

About de materials and resources origins, no fresh hardware purchases were made. I relied on the Viennese HPC center's existing infrastructure, which follows European directives on responsible energy usage and publishes annual reports discussing sustainability practices. *PennyLane* itself is developed by a community that strives for ethical and

transparent technology, so both the HPC resources and the software align with these principles.

The emissions calculations are detailed below:

Laptop emissions:

$$E_{\mathrm{l}} = P_{\mathrm{laptop}} \cdot t_{\mathrm{laptop}} \cdot \mathrm{EF}_{\mathrm{electricity}} = 0.03\,\mathrm{kW} \cdot 540\,\mathrm{h} \cdot 0.25\,\mathrm{kg\ CO_2/kWh} = 4.05\,\mathrm{kg\ CO_2}$$

Server emissions:

$$E_{\mathrm{s}} = P_{\mathrm{server}} \cdot t_{\mathrm{server}} \cdot \mathrm{EF}_{\mathrm{electricity}} = 0.2\,\mathrm{kW} \cdot 540\,\mathrm{h} \cdot 0.25\,\mathrm{kg\ CO_2/kWh} = 27.0\,\mathrm{kg\ CO_2}$$

Transport emissions:

$$E_{\mathrm{t}} = d_{\mathrm{metro}} \cdot n_{\mathrm{days}} \cdot \mathrm{EF}_{\mathrm{metro}} = 3.5\,\mathrm{km} \cdot 120\,\mathrm{days} \cdot 0.014\,\mathrm{kg\ CO_2/km} = 1.68\,\mathrm{kg\ CO_2}$$

Total emissions:

$$E_{\mathrm{total}} = E_{\mathrm{l}} + E_{\mathrm{s}} + E_{\mathrm{t}} = 4.05\,\mathrm{kg\ CO_2} + 27.0\,\mathrm{kg\ CO_2} + 1.68\,\mathrm{kg\ CO_2} = 32.73\,\mathrm{kg\ CO_2}$$

Execution

Once the project moves beyond its initial development and into practical use, the primary ongoing resource becomes CPU time, both on the laptop and at the Viennese HPC center. I anticipate an annual energy consumption in the range of 500 kWh for active simulations, leading to approximately 75 kg of CO_2 if the current power mix remains the same. However, because the HPC center integrates some lower-carbon energy sources, there is hope that the carbon intensity of these computations could decrease over time.

One of the key advantages of leveraging quantum approaches is the possibility of reducing the energy used in large-scale calculations. Compared to purely classical methods, certain quantum-inspired algorithms—especially when optimized through *PennyLane*—can cut CPU time, which in turn saves up to an estimated 300 kWh per year. This reduction lowers both energy costs and carbon emissions.

At the conclusion of the project, as it is primarily a digital endeavor, no physical waste is generated. Upon completion, the data can be either archived or securely deleted, requiring minimal energy consumption and resulting in an almost negligible environmental footprint. Relying on renewable energy within the HPC center, continuing to refine algorithms, and scaling down usage when computational tasks are not urgent could all reduce the overall footprint further.

Emissions calculations:

Annual energy consumption emissions:

$$E_{\text{annual}} = E_{\text{cpu}} \cdot \text{EF}_{\text{electricity}} = 500\,\text{kWh} \cdot 0.15\,\text{kg CO}_2/\text{kWh} = 75\,\text{kg CO}_2$$

Potential savings from quantum optimization:

$$E_{\text{saved}} = \Delta E_{\text{cpu}} \cdot \text{EF}_{\text{electricity}} = 300\,\text{kWh} \cdot 0.15\,\text{kg CO}_2/\text{kWh} = 45\,\text{kg CO}_2$$

Net emissions with optimization:

$$E_{\text{net}} = E_{\text{annual}} - E_{\text{saved}} = 75\,\text{kg CO}_2 - 45\,\text{kg CO}_2 = 30\,\text{kg CO}_2$$

Risks and Limitations

Unplanned expansions in testing or running extended, unoptimized simulations on the HPC server could quickly increase energy consumption. Without proper scheduling or oversight, the footprint could grow significantly. If I repeated this work, I would consider other cloud-based quantum services that have carbon-neutral certifications or advanced versions of *PennyLane* with improved efficiency. Tight scheduling of simulations to off-peak energy hours could also help. Key figures rely on average emission factors, and the power mix of the HPC center can change. Precise measurements for every hour of server usage are challenging, which introduces uncertainty into the calculations.

5.1.2 Economic Perspective

Development Costs

The development phase of the project incurred various expenses related to labor, energy consumption, workspace operations, supervision, transportation, and travel. Labor was the primary cost, with 540 hours of work valued at 25 €/hour, amounting to a significant portion of the budget. Energy consumption included the electricity required to power a Mac laptop with a 30 W average consumption and the high-performance computing (HPC) server at the Viennese research center, which operates at approximately 200 W during heavy workloads. Additionally, the workspace used for development consumed energy beyond computing devices, including lighting and heating.

Supervision of the project involved bi-weekly one-hour meetings with two professors over the course of five months, which added to the overall cost due to their expertise and hourly rate. Transportation costs included daily commuting for 120 days, as well as mobility expenses estimated at 983 €/month for five months. Furthermore, the project required two round-trip flights, each costing 120 €, to attend important meetings and consultations.

To reduce costs during the development phase, I utilized existing resources, including a Mac laptop and free access to the HPC server at the Viennese research center, avoiding the purchase of new hardware or renting commercial cloud computing services. Open-

source software like *PennyLane* was used to eliminate licensing fees, and simulations were carefully planned to minimize idle time on the HPC server and optimize energy consumption. Transportation costs were managed by relying on public transit for daily commuting and limiting flights to essential project phases. Supervision costs were optimized by holding concise, bi-weekly meetings with professors to ensure productive feedback.

Labor costs:

$$C_{\text{labor}} = t_{\text{hours}} \cdot \text{Rate}_{\text{labor}} = 540\,\text{hours} \cdot 25\,€/\text{hour} = 13,500\,€$$

Energy consumption costs:

$$C_{\text{energy}} = E_{\text{consumed}} \cdot \text{Rate}_{\text{electricity}} = 108\,\text{kWh} \cdot 0.18\,€/\text{kWh} = 19.44\,€$$

HPC commercial equivalent:

$$C_{\text{HPC}} = t_{\text{hours}} \cdot \text{Rate}_{\text{HPC}} = 540\,\text{hours} \cdot 0.5\,€/\text{hour} = 270\,€$$

Workspace energy consumption:

$$C_{\text{workspace}} = E_{\text{workspace}} \cdot \text{Rate}_{\text{electricity}} = 220.5\,\text{kWh} \cdot 0.18\,€/\text{kWh} = 39.69\,€$$

Transport costs:

$$C_{\text{transport}} = C_{\text{monthly}} \cdot n_{\text{months}} = 983\,€/\text{month} \cdot 5\,\text{months} = 4,915\,€$$

Supervisor costs:

$$C_{\text{supervisors}} = n_{\text{supervisors}} \cdot t_{\text{meetings}} \cdot \text{Rate}_{\text{supervisor}} = 2 \cdot 10\,\text{hours} \cdot 50\,€/\text{hour} = 1,000\,€$$

Flight costs:

$$C_{\text{flights}} = n_{\text{flights}} \cdot \text{Rate}_{\text{flight}} = 2 \cdot 120\,€ = 240\,€$$

Total costs:

$$C_{\text{total}} = 19,984.13\,€$$

This detailed breakdown highlights the various expenses associated with the project, ensuring that all relevant components are accounted for. The final total cost for the development phase amounts to approximately 19,984.13 €.

Execution

If the project remains active and consumes around 500 kWh annually, it would cost an additional 90 € per year (at 0.18 €/kWh). Improved energy prices or algorithmic

refinements could further lower this expense.

Most maintenance revolves around software updates, bug fixes, and code improvements, which involve minimal monetary outlays. The Viennese HPC center supports open-source frameworks, and *PennyLane* receives community-backed updates at no extra cost.

Since the project is entirely digital, shutting it down incurs negligible expense. Data can be archived or securely deleted, and no physical equipment needs special handling.

Any quantum simulation tools or modules developed here could assist future research, decreasing start-up costs and encouraging interdisciplinary collaboration. The open approach ensures that others can build on these methods freely.

Risks and Limitations

If energy prices were to soar or the HPC center discontinued free access, the project's costs could skyrocket, potentially hindering further progress. Additionally, if the project expands and requires more resources, the expenses could increase significantly.

Estimates rely on current prices and the stable availability of HPC resources. Rapid market changes, especially in energy, might invalidate long-term cost projections. Furthermore, technological obsolescence poses a risk, as outdated hardware or software could necessitate costly upgrades or replacements. This issue is particularly relevant for cutting-edge quantum simulations that depend on advanced computational infrastructure.

Another potential risk involves changes in funding or policy frameworks. If institutional or governmental support for quantum research diminishes, securing alternative resources could become challenging. This could introduce delays or even jeopardize the continuation of the project entirely. These risks highlight the importance of regular evaluations and contingency planning to ensure sustainability.

5.1.3 Social Perspective

Development

Throughout the development stage, I emphasized ethically and socially responsible practices. This included using clear, inclusive language in all documentation and making the core results openly accessible. Given that quantum computing is a pioneering area with potential global impact, I aimed to set a collaborative tone and steer clear of any design choices that might discriminate against particular user groups.

The Viennese HPC center publishes regular reports outlining its commitment to responsible energy use and fair resource distribution. Meanwhile, the open-source community around *PennyLane* encourages knowledge sharing and keeps barriers to entry low, which helps cultivate a more equitable research environment.

Execution

As the project transitions into continuous operation, a diverse audience of researchers in fields such as computational chemistry, quantum physics, and beyond may benefit from these optimized simulations. Users anywhere in the world can deploy the code, provided they have sufficient HPC access, and the open documentation helps ensure they understand and can modify the methodology. However, disparities in HPC availability could widen the gap between institutions that can leverage quantum resources effectively and those that cannot.

In addressing the original challenge of achieving faster, more efficient simulations, the solution outlined here has proven successful. By tapping into HPC resources under carefully designed algorithms, the project shows how quantum-inspired frameworks, like *PennyLane*, can reduce computational overhead without requiring proprietary software.

Risks and Limitations

A key concern relates to uneven access. If HPC centers are concentrated in a few regions, researchers in other parts of the world may struggle to replicate results or remain competitive. Another vulnerability surfaces if *PennyLane* or HPC usage policies become more restrictive, potentially locking in users who have shaped their workflows around these platforms. Finally, it is worth noting that this social analysis assumes relatively stable conditions that may not always apply to low-income or remote communities, where internet connectivity and funding are limited.

5.2 Ethical Implications

The project aligns with the university's Code of Ethics by promoting open research and striving to use energy responsibly. Quantum computing carries the potential to transform a wide range of scientific activities, so I made sure to prioritize transparency, collaboration, and accessibility. Each phase of the work underscores an intention to minimize harmful applications, support inclusive participation, and encourage responsible innovation that extends benefits to the broader community.

5.3 Relation to the Sustainable Development Goals (SDGs)

- **Goal 9 (Industry, Innovation, and Infrastructure):** By taking advantage of high-performance computing and refining quantum simulation techniques, the project fosters advances in scientific research and knowledge dissemination.
- **Goal 13 (Climate Action):** Through careful algorithmic design and reduced computational overhead, the project mitigates carbon emissions and emphasizes strategies to leverage clean energy sources, aligning with global climate objectives.

CHAPTER 6

Conclusions and Future Work

6.1 Conclusions

In this project, we have successfully implemented a quantum simulator focused on simulating various molecular systems using the VQE algorithm. The results demonstrate the ability to optimize the processes for H_2, LiH, and H_2O, molecules of different sizes and complexities. Additionally, the efficacy of the UCCSD ansatz has been validated, achieving superior results compared to other ansätze. An unexpected outcome, which significantly enhances the value of our project, was demonstrating that, for our implementation, the *autograd* interface outperforms JAX.

The contributions of this work to the field include the modular design of quantum simulation software, enabling extensibility and flexibility for future algorithms and optimization strategies. Furthermore, the introduction of an adaptive methodology for selecting different ansätze and optimizers has made the optimization process more efficient and faster.

Consequently, the objectives of our project have been successfully achieved. These objectives include the development of an adaptive ansatz capable of selecting the operators with the greatest impact on the system, the integration of a hybrid optimization approach that adjusts both the ansatz parameters and nuclear positions, and endows our simulations with greater robustness and precision. Finally, the design of a modular architecture facilitates the inclusion of new types of ansätze and optimizers, enabling the comparison of different optimization strategies for future research.

6.2 Future Directions

In this project, the initial questions posed have been successfully addressed. However, after the completion of the project, new frontiers and research lines have emerged, offering exciting opportunities for future work.

During the development of the project, the hybrid optimization methodology could be

further refined by adding to the optimization process, thereby achieving greater efficiency in convergence. We realized that another viable option to enhance simulation convergence would be to implement an adaptive optimization system, which dynamically adjusts the number of optimizations of the ansatz parameters based on the simulation's progress. This would result in greater efficiency in the simulation's convergence. Moreover, it was observed that automating the configuration of optimizers would save considerable time during setup.

As a final future endeavor, to improve the simulator's consistency, it would be valuable to investigate its performance on NISQ systems. This would enable analyzing whether implementing a noise model affects the simulation's convergence, thus validating the robustness of the simulator in real-world quantum systems.

Another relevant research avenue would involve integrating error mitigation techniques, such as zero-noise extrapolation, to enhance the accuracy of simulations on noisy quantum devices. This would add greater realism to the simulations and make the simulator more practical for applications on current quantum hardware.

Finally, given the simulator's modular structure, it could be extended to other fields beyond chemistry, such as material science and condensed matter physics. Exploring these areas would broaden its impact and leverage its flexibility for a wide range of scientific applications.

Bibliography

The *biblatex* system simplifies the management of the bibliography in scientific works, providing automation and customization in the format of citations. This allows the document's author to focus on the content without having to worry about the style of the references, saving time and reducing errors.

The bibliographic references database is in the file "TFG.bib", and this is where you should add your references. Consult the `biblatex` manual, section "Database Guide", to learn about the available types of references and fields.

You can modify (or delete) this note by editing the `\defbibnote` macro in the file "TFG.tex".

---

[1] Nacer Eddine Belaloui et al. "Ground State Energy Estimation on Current Quantum Hardware Through The Variational Quantum Eigensolver: A Comprehensive Study". In: *arXiv preprint arXiv:2412.02606* (2024).

[2] J. Ignacio Cirac et al. "Matrix Product States and Projected Entangled Pair States: Concepts, Symmetries, and Theorems". In: *arXiv* (2020). Discusses MPS and PEPS techniques for representing and simulating quantum systems efficiently., pp. 14–15. URL: https://arxiv.org/abs/2011.12127.

[3] PennyLane Developers. *qml.QNGOptimizer — PennyLane 0.39.0 documentation*. Accessed: January 14, 2025. 2025. URL: https://docs.pennylane.ai/en/stable/code/api/pennylane.QNGOptimizer.html.

[4] I. M. Georgescu, S. Ashhab, and Franco Nori. "Quantum Simulation". In: *Reviews of Modern Physics* 86 (2014), p. 41. DOI: 10.1103/RevModPhys.86.153. arXiv: 1308.6253 [quant-ph]. URL: https://arxiv.org/abs/1308.6253.

[5] Gabriel Greene-Diniz and David Muñoz Ramo. "Generalized Unitary Coupled Cluster Excitations for Multireference Molecular States Optimized by the Variational Quantum Eigensolver". In: *arXiv preprint arXiv:1910.05168* (2019). URL: https://arxiv.org/abs/1910.05168.

[6] Harper R. Grimsley et al. "ADAPT-VQE: An Adaptive Variational Algorithm for Quantum Chemistry". In: *Nature Communications* (2019). DOI: 10.1038/s41467-

019-10988-2. arXiv: 1812.11173 [quant-ph]. URL: https://arxiv.org/pdf/1812.11173.

[7] *Hamiltonian (quantum mechanics)*. https://en.wikipedia.org/wiki/Hamiltonian_(quantum_mechanics). Last accessed: December 20, 2024.

[8] Dominik Hangleiter, Jacques Carolan, and Karim P. Y. Thébault. *Analogue Quantum Simulation: A New Instrument for Scientific Understanding*. 2023. DOI: 10.1007/978-3-030-87216-8. arXiv: 2303.00814 [quant-ph]. URL: https://arxiv.org/abs/2303.00814.

[9] *Hartree–Fock method*. Last accessed: January 9, 2025. URL: https://en.wikipedia.org/wiki/Hartree%E2%80%93Fock_method.

[10] IBM Quantum. *Quantum Computing Topics*. Accessed: 2025-01-14. 2025. URL: https://www.ibm.com/think/topics/quantum-computing.

[11] Ankit Kumar et al. "Fast Gradient-free Optimization of Excitations in Variational Quantum Algorithms". In: *arXiv preprint arXiv:2409.05939* (2024). URL: https://arxiv.org/pdf/2409.05939.

[12] Wim Lavrijsen et al. "Classical Optimizers for Noisy Intermediate-Scale Quantum Devices". In: *arXiv preprint arXiv:2004.03004* (2020). URL: https://arxiv.org/abs/2004.03004.

[13] Alberto Peruzzo et al. "A variational eigenvalue solver on a photonic quantum processor". In: *Nature Communications* 5 (2014), p. 4213. DOI: 10.1038/ncomms5213. URL: https://arxiv.org/pdf/1304.3061.

[14] Stefano Pirandola et al. "Advances in Quantum Teleportation". In: *Nature Photonics* 9.10 (2015), pp. 641–652. DOI: 10.1038/nphoton.2015.154. URL: https://doi.org/10.1038/nphoton.2015.154.

[15] *Post-Hartree-Fock*. Last accessed: January 9, 2025. URL: https://en.wikipedia.org/wiki/Post%E2%80%93Hartree%E2%80%93Fock.

[16] IBM Quantum. *Variational Quantum Eigensolver Tutorial*. https://learning.quantum.ibm.com/tutorial/variational-quantum-eigensolver. Last accessed: January 8, 2025.

[17] Sebastian Ruder. "An overview of gradient descent optimization algorithms". In: *arXiv preprint arXiv:1609.04747* (2016). URL: https://arxiv.org/pdf/1609.04747.

[18] Kyle M. Sherbert et al. "Parameterization and optimizability of pulse-level VQEs". In: *arXiv preprint arXiv:2405.15166* (2024). Last accessed: January 8, 2025. URL: https://arxiv.org/pdf/2405.15166.

[19] Kenji Sugisaki et al. "Size-consistency and Orbital-invariance Issues Revealed by VQE-UCCSD Calculations with the FMO Scheme". In: *arXiv preprint arXiv:2402.17993* (2024). URL: https://arxiv.org/abs/2402.17993.

[20] Terence Tao. “The Schrödinger Equation”. Available at https://www.math.ucla.edu/~tao/preprints/schrodinger.pdf. Mar. 2006.

[21] Jules Tilly et al. “The Variational Quantum Eigensolver: a review of methods and best practices”. In: *arXiv preprint arXiv:2111.05176* (2021).

[22] Wikipedia contributors. *Qubit*. Last accessed: January 8, 2025. 2025. URL: https://en.wikipedia.org/wiki/Qubit.

[23] Saad Yalouz et al. “Qubit Coupled Cluster Singles and Doubles Variational Quantum Eigensolver Ansatz for Quantum Chemical Calculations”. In: *arXiv preprint arXiv:2005.08451* (2020). URL: https://arxiv.org/abs/2005.08451.

[24] Nick Yoder. *Moore’s Law and Quantum Computers*. 2023. URL: https://nickyoder.com/moores-law-quantum-computer/.

[25] Atsushi Yoshikawa et al. “Towards Accurate Quantum Chemical Calculations on Noisy Quantum Computers”. In: *arXiv preprint arXiv:2311.09634* (2023). URL: https://arxiv.org/pdf/2311.09634.

[26] Yu Zhang et al. “Optimizing Quantum Programs against Decoherence: Delaying Qubits into Quantum Superposition”. In: *Proceedings of the 13th International Symposium on Theoretical Aspects of Software Engineering (TASE)*. 2019, doi:10.1109/TASE.2019.000–2. eprint: arXiv:1904.09041. URL: https://arxiv.org/abs/1904.09041.

[27] Wojciech H. Zurek. “Decoherence and the Transition from Quantum to Classical – REVISITED”. In: *arXiv preprint quant-ph/0306072* (2003). URL: https://arxiv.org/pdf/quant-ph/0306072.

APPENDIX A

Logic Gates

A.1 Simple Logic Gates

Below are detailed the simple logic gates essential for constructing more complex quantum algorithms:

X Gate (Pauli-X) The **Pauli-X** gate is the quantum analog of the classical NOT gate. It performs a bit flip on the qubit, transforming the state $|x\rangle$ into $|\neg x\rangle$.

Representative Matrix

$$X = \begin{pmatrix} 0 & 1 \\ 1 & 0 \end{pmatrix}$$

Effect on Basis States

- $X|0\rangle = |1\rangle$
- $X|1\rangle = |0\rangle$

Y Gate (Pauli-Y) The **Pauli-Y** gate performs a rotation of π around the y-axis. It transforms the state $|x\rangle$ into $i(-1)^x|\neg x\rangle$.

Representative Matrix

$$Y = \begin{pmatrix} 0 & -i \\ i & 0 \end{pmatrix}$$

Effect on Basis States

- $Y|0\rangle = i|1\rangle$
- $Y|1\rangle = -i|0\rangle$

Z Gate (Pauli-Z) The **Pauli-Z** gate is known as the phase inversion gate. It transforms the state $|x\rangle$ into $(-1)^x|x\rangle$.

Representative Matrix

$$Z = \begin{pmatrix} 1 & 0 \\ 0 & -1 \end{pmatrix}$$

Effect on Basis States

- $Z|0\rangle = |0\rangle$
- $Z|1\rangle = -|1\rangle$

Hadamard Gate (H) The **Hadamard** gate creates an equal superposition of the computational basis states. It transforms the state $|x\rangle$ into $\frac{1}{\sqrt{2}}(|0\rangle + (-1)^x|1\rangle)$.

Representative Matrix

$$H = \frac{1}{\sqrt{2}} \begin{pmatrix} 1 & 1 \\ 1 & -1 \end{pmatrix}$$

Effect on Basis States

- $H|0\rangle = \frac{1}{\sqrt{2}}(|0\rangle + |1\rangle) = |+\rangle$
- $H|1\rangle = \frac{1}{\sqrt{2}}(|0\rangle - |1\rangle) = |-\rangle$

A.2 Multi-Qubit Logic Gates

Controlled-NOT Gate (CNOT) The **CNOT** or **Controlled-X** gate is a two-qubit gate that flips the second qubit (target) if and only if the first qubit (control) is in the state $|1\rangle$. It transforms the state $|x, y\rangle$ into $|x, x \oplus y\rangle$, where $\oplus$ denotes the XOR operation.

Representative Matrix

$$\text{CNOT} = \begin{pmatrix} 1 & 0 & 0 & 0 \\ 0 & 1 & 0 & 0 \\ 0 & 0 & 0 & 1 \\ 0 & 0 & 1 & 0 \end{pmatrix}$$

Effect on Basis States

- $\text{CNOT}|00\rangle = |00\rangle$
- $\text{CNOT}|01\rangle = |01\rangle$
- $\text{CNOT}|10\rangle = |11\rangle$
- $\text{CNOT}|11\rangle = |10\rangle$

Single Excitation Gate (*SingleExcitation*) This gate performs a rotation in the two-dimensional subspace $\{|01\rangle, |10\rangle\}$. It transforms the state $|10\rangle$ into $\cos\left(\frac{\phi}{2}\right)|10\rangle - \sin\left(\frac{\phi}{2}\right)|01\rangle$.

Representative Matrix	Effect on Basis States
$U(\phi) = \begin{pmatrix} 1 & 0 & 0 & 0 \\ 0 & \cos\left(\frac{\phi}{2}\right) & -\sin\left(\frac{\phi}{2}\right) & 0 \\ 0 & \sin\left(\frac{\phi}{2}\right) & \cos\left(\frac{\phi}{2}\right) & 0 \\ 0 & 0 & 0 & 1 \end{pmatrix}$	It affects the subspace $\{\|01\rangle, \|10\rangle\}$, performing a rotation parameterized by ϕ.

Double Excitation Gate (*DoubleExcitation*) This gate performs a rotation in the subspace of states $\{\|0011\rangle, \|1100\rangle\}$. It specifically affects these states, leaving the others unchanged.

Representative Matrix	Effect on Basis States
$U(\phi) = \begin{pmatrix} I_{12} & 0 & 0 \\ 0 & \begin{pmatrix} \cos\left(\frac{\phi}{2}\right) & -\sin\left(\frac{\phi}{2}\right) \\ \sin\left(\frac{\phi}{2}\right) & \cos\left(\frac{\phi}{2}\right) \end{pmatrix} & 0 \\ 0 & 0 & I_2 \end{pmatrix}$	It performs a rotation parameterized by ϕ in the subspace $\{\|0011\rangle, \|1100\rangle\}$.

These gates are implemented in PennyLane as `qml.SingleExcitation` and `qml.DoubleExcitation`, and are essential in quantum chemistry algorithms such as the *Unitary Coupled-Cluster Singles and Doubles* (UCCSD).